

Fast and Interpretable Mortality Risk Scores for Critical Care Patients

Chloe Qinyu Zhu[†], Muhang Tian[†], Lesia Semenova, Jiachang Liu,
Jack Xu, Joseph Scarpa, Cynthia Rudin*
Department of Computer Science, Duke University

Abstract

Prediction of mortality in intensive care unit (ICU) patients is an important task in critical care medicine. Prior work in creating mortality risk models falls into two major categories: domain-expert-created scoring systems, and black box machine learning (ML) models. Both of these have disadvantages: black box models are unacceptable for use in hospitals, whereas manual creation of models (including hand-tuning of logistic regression parameters) relies on humans to perform high-dimensional constrained optimization, which leads to a loss in performance. In this work, we bridge the gap between accurate black box models and hand-tuned interpretable models. We build on modern interpretable ML techniques to design accurate and interpretable mortality risk scores. We leverage the largest existing public ICU monitoring datasets, namely the MIMIC III and eICU datasets. By evaluating risk across medical centers, we are able to study generalization across domains. In order to customize our risk score models, we develop a new algorithm, `GROUPFASTERRISK`, which has several important benefits: (1) it uses hard sparsity constraint, allowing users to directly control the number of features; (2) it incorporates group sparsity to allow more cohesive models; (3) it allows for monotonicity correction on models for including domain knowledge; (4) it produces many equally-good models at once, which allows domain experts to choose among them. `GROUPFASTERRISK` creates its risk scores within hours, even on the large datasets we study here. `GROUPFASTERRISK`'s risk scores perform better than risk scores currently used in hospitals, and have similar prediction performance to black box ML models (despite being much sparser). Because `GROUPFASTERRISK` produces a variety of risk scores and handles constraints, it allows *design flexibility*, which is the key enabler of practical and trustworthy model creation.

1 Introduction

Prediction of in-hospital mortality risk is a crucial task in medical decision-making [1–3], assisting medical practitioners to better estimate the patient’s state and allocate resources appropriately for better treatment, disease staging, and triage support [4–6]. Mortality risk is usually performed with *severity of illness risk scores*, where each feature is transformed into an integer-valued component function based on its degree of deviation from normal values, and a nonlinear function transforms the sum of component functions into an estimate of risk. Risk scores are designed to be easy to understand, troubleshoot, and use in practice. A method for constructing more accurate (but still interpretable) severity of illness risk scores could save lives and assist with better allocation of resources.

The severity of illness risk scores have been constructed in various ways since the early 1980’s, starting with the APACHE [7], SOFA [8, 9], APACHE II [10], and SAPS [11] scores, which are still in use presently, as well as the more recent APACHE IV [12] score. All of these scores were built using a combination of basic statistical techniques and domain expertise. Statistical hypothesis testing was generally used for variable selection, and techniques like logistic regression and locally weighted least squares [13] were often used for combining variables. This process left many manual choices for analysts: at what significance level should we stop including variables? Of the many features selected by hypothesis testing, how should we choose which ones would be included? How should the cutoffs for risk increases for each variable be determined? How do the risk scores from logistic regression become integer point values that doctors can easily sum, troubleshoot, and understand? While a variety of heuristics have been used to answer these

[†]Equal contribution. *Corresponding author.

questions, ideally, the answers would be determined automatically by an algorithm that optimizes predictive performance; humans, even equipped with heuristics, are not naturally adept at high-dimensional constrained optimization. It is particularly important that these models are *sparse* in the number of features so they are easy to calculate in practice. For instance, because APACHE scores require 142 features, they are potentially more error-prone, and not all features may be available for every patient.

Recently, more modern statistical and machine learning (ML) approaches have been used to create interpretable models for predicting mortality without the need for manual intervention. Specifically, the OASIS score [14] was built from a process consisting of a genetic algorithm [15] that selects a subset of predictive variables to be included in the system, particle swarm optimization [16] to determine integer scores for each decile of the variables, and logistic regression for transforming integer scores into probability predictions. However, genetic algorithm and particle swarm optimization approaches can be insufficient, leading to the possibility of improved performance using other techniques.

State-of-the-art black box ML approaches have been applied to the mortality risk prediction, aiming to improve predictive performance [17–22]. For instance, OASIS+ researchers [18] used a variety of black box ML algorithms (such as random forest [23] and XGBoost [24]) on OASIS features to develop models that mostly outperform other severity of illness scores such as OASIS and SAPS II. The black box models combine variables in highly nonlinear ways, and are not easy to troubleshoot or use in practice, which is why, to the best of our knowledge, OASIS+ models have not been adopted for mortality risk prediction in ICUs. Black box models with “explanations” are also insufficient [25]. However, it is useful to benchmark with black box models to determine whether there is a gap in accuracy between interpretable and black box models. In this work, we also benchmark against black box accuracy and show that our new techniques are able to close the gap.

In this work, we introduce `GROUPFASTERRISK`— an interpretable machine learning algorithm capable of producing a set of diverse, high-quality risk scores with equally high predictive accuracy — to generate severity of illness scores. `GROUPFASTERRISK` automates feature selection, cutoffs for risk increases, and integer weight assignments. Our approach optimizes more carefully than the approach of OASIS and another risk-score generation method called `AutoScore` [26], is much more scalable than its predecessor `RiskSLIM` [27, 28], and is more customizable than its predecessor `FasterRisk` [29]. `GROUPFASTERRISK` optimization process yields higher-quality interpretable models than competitors; in fact, its models are as predictive as black box models. Our contributions are as follows:

- We propose a new framework, namely `GROUPFASTERRISK`, for the automatic creation of severity of illness scores using an ML algorithm. `GROUPFASTERRISK` produces accurate risk scores within a relatively short time on a small personal laptop while giving users the flexibility to use an arbitrary number of physiological measurements and sparsity constraints. `GROUPFASTERRISK` incorporates group sparsity and monotonicity constraints in its optimization process to allow for the creation of more cohesive and interpretable models for medical applications.
- Using `GROUPFASTERRISK`, we provide multiple high-quality mortality risk scores with varying sparsity constraints and a number of variables, which could be potentially applied in a critical care setting to provide mortality risk predictions.
- Through extensive out-of-distribution (OOD) testing (at hospitals not used for training), we demonstrate that risk scores created by `GROUPFASTERRISK` outperform OASIS and SAPS II and are similar in performance to APACHE IV/IVa while using much fewer variables, thus being much easier to troubleshoot and use. Results also demonstrate that our approach generalizes OOD and even performs similarly to black box ML models.
- Our proposed method performs well across subpopulations, exceeding the performance of OASIS and SOFA on sepsis/septicemia patients, acute myocardial infarction patients, heart failure patients, and acute kidney failure patients. Its scores are comparable to SAPS II and APACHE IV, exceeding their performance in some subpopulations.
- We show that `GROUPFASTERRISK` selects more useful features than OASIS for predicting patient outcomes. We also show that it produces fair and well-calibrated predictions across different ethnic and gender groups across the United States.

Sparsity Evaluation Metric: We define a model’s sparsity informally as a way of measuring the model’s size. For linear models such as logistic regression, explainable boosting machine (EBM) [33], AutoScore [26], and GROUPFASTERRISK, sparsity is the total number of coefficients, intercepts, and multipliers. For tree-based models like XGBoost [34], AdaBoost [35], and Random Forest [23], sparsity is the number of splits in all trees.

Calibration Evaluation Metrics: In mortality risk prediction, even if a model demonstrates high accuracy based on AUROC and AUPRC, it may not provide precise risk probability estimates. This is because they are rank statistics [36]. We evaluate reliability based on *Brier score*, *Hosmer-Lemeshow χ^2 statistics* (HL χ^2), and the *standardized mortality ratio* (SMR) [37, 38]. We use *C-statistics* for HL χ^2 , calculated from deciles of predicted probabilities. Unless mentioned otherwise, we use paired *t*-test for statistical testing, and the *p*-value is denoted with *p*.

2.1.2 GROUPFASTERRISK and Baseline Methods used for Comparison

GROUPFASTERRISK produces high-quality risk scores. It improves over its predecessor FasterRisk [29], which is a data-driven ML approach that learns high-quality scoring systems within a relatively short time (Figure 4b). Although FasterRisk achieves near-optimal performance, it has limitations: (1) it does not allow users to add hard constraints on the number of features used in the model; (2) it does not incorporate monotonicity constraints, which means it can learn unrealistic component functions (see examples of ablation study in Appendix C.1). To handle (1) and (2), GROUPFASTERRISK includes *group sparsity* and *monotonicity correction*. The group sparsity option allows users to define any arbitrary partition (grouping) of the features and regularize all of these features towards 0 simultaneously. The monotonicity correction ensures that the models are nondecreasing (or nonincreasing) along one variable. GROUPFASTERRISK then produces multiple diverse, equally accurate models obeying this constraint. The trained models could be easily visualized with a risk scorecard representation using our software. We discuss group sparsity and monotonic correction in Methods (Section 4.1 and Section 4.4 correspondingly).

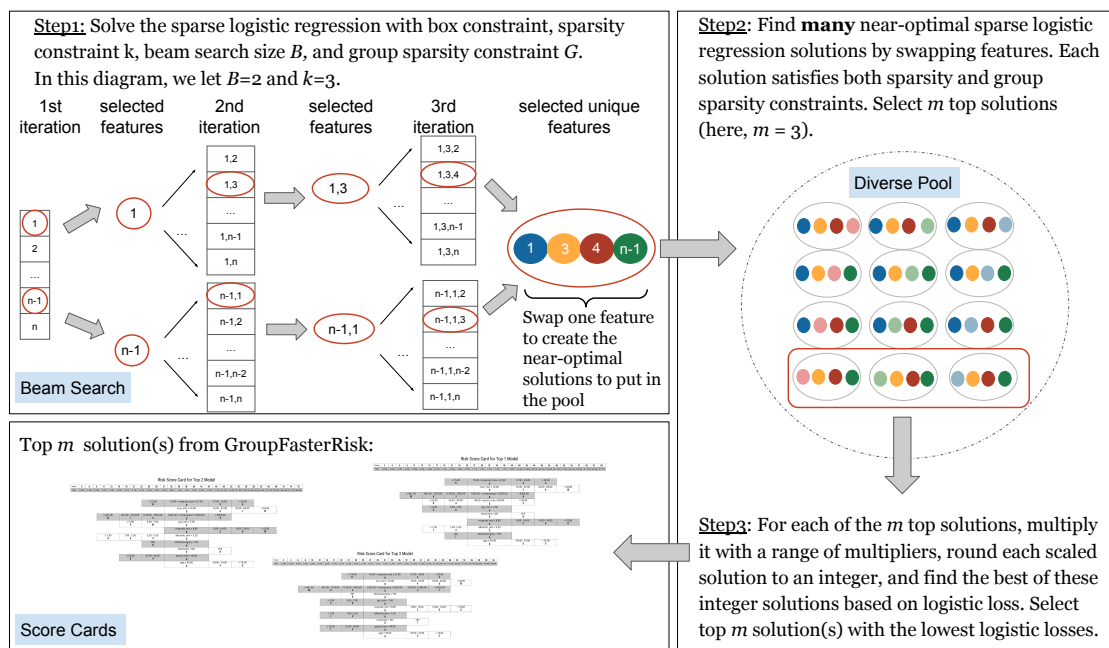


Figure 2: GROUPFASTERRISK algorithm workflow. We first find a near-optimal solution for a sparse logistic regression problem without the integer constraints. This solution is used in the second stage to search for a diverse pool of sparse continuous solutions that also satisfy various constraints (still ignoring the integer constraints) while having similar predictive accuracy. We subsequently select the top m solutions and apply a rounding search subroutine to obtain integer-valued solutions. Our algorithm is carefully designed to ensure that the integer-valued solutions maintain similar performance to real-valued solutions.

Figure 2 summarizes the algorithmic approach of `GROUPFASTERRISK`, which returns scorecard displays in three steps. We begin by solving the sparse logistic regression problem, producing a near-optimal, real-valued sparse solution. This single solution is then used to find multiple diverse solutions with similar logistic loss [39–41]). Finally, a rounding subroutine is applied to all solutions to transform real-valued coefficients into integers, creating multiple risk scorecards that practitioners can choose from. Monotonicity correction can be optionally incorporated in all three steps. Notably, compared to other scoring system methods, `GROUPFASTERRISK` can produce high-quality risk scores for MIMIC III within a few hours on a personal laptop (we discuss more on the run time of `GROUPFASTERRISK` in Section 2.2).

To demonstrate the superiority of our proposed method, we compare it with two sets of baselines. The first set includes existing severity of illness scores such as the Oxford Acute Severity of Illness Score (OASIS) [14], Simplified Acute Physiology Score II (SAPS II) [42], Sequential Organ Failure Assessment (SOFA) [8], and Acute Physiology and Chronic Health Evaluation IV/IVa (APACHE IV/IVa) [12]. We did not consider qSOFA [9] because the score was originally developed for organ failure assessment, which may not directly predict in-hospital mortality. However, studies [43] have shown that SOFA can outperform qSOFA on in-hospital mortality prediction tasks, so we include SOFA. The second set of baselines consists of widely used ML algorithms, such as Logistic Regression, EBM [44], Random Forest [23], AdaBoost [35], and XGBoost [24]. (A predecessor of `GROUPFASTERRISK` is RiskSLIM [27, 28], which has been tested extensively with `FasterRisk`, so we do not include it here as it is much more computationally expensive.) We further categorize these baselines into two groups based on the number of variables: sparse (no more than 17 variables, including OASIS, SOFA, and SAPS II) and not sparse (more than 40 variables, like APACHE IV/IVa). Our goal is to develop sparse models since they are highly interpretable [39], but we still evaluate `GROUPFASTERRISK` models against APACHE IV/IVa. For fair comparison, we set the same or lower group sparsity constraint (number of variables) on `GROUPFASTERRISK` than the baselines across all the experiments. For conciseness, we denote `GROUPFASTERRISK` models with the prefix GFR and group sparsity as the suffix. For instance, a `GROUPFASTERRISK` model trained with a group sparsity of 10 is GFR-10.

2.2 All-cause Mortality Prediction

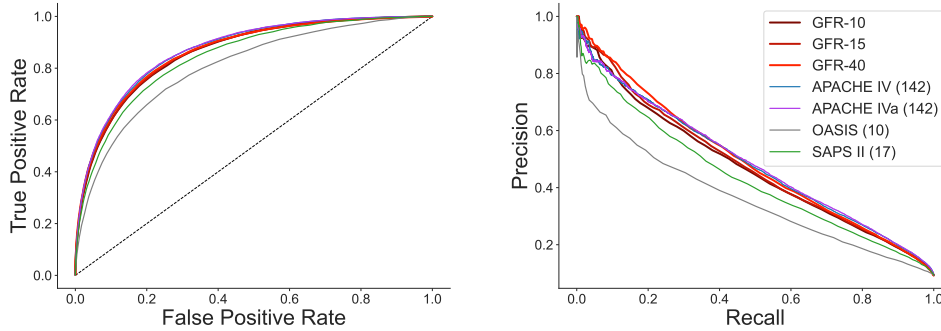
We first focus on evaluating how `GROUPFASTERRISK` performs, in terms of predictive performance and sparsity, when predicting all-cause in-hospital mortality. We further consider patients with different critical illnesses in Section 2.3.

In-Distribution Performance: Our results in Figure 3b show that `GROUPFASTERRISK` predicted in-hospital mortality with the best AUROC and AUPRC across all internal evaluations on MIMIC III test folds. Specifically, GFR-10 achieves an AUROC of 0.813 (± 0.007) and AUPRC of 0.368 (± 0.011), around 0.05 higher than OASIS. When using fifteen features, GFR-15 achieves an AUROC of 0.836 (± 0.006) and AUPRC of 0.403 (± 0.011), both around 0.05 higher than SAPS II (all the reported results are statistically significant with $p < 0.001$).

Sparsity: We observe that `GROUPFASTERRISK` models are less complex than the competing scoring systems (Figure 3b). Indeed, when using ten features, GFR-10 has model complexity of 42 (± 0) whereas OASIS has 47. For fifteen features, GFR-15 is 48 (± 4.9) while SAPS II is 58. Our results indicate that `GROUPFASTERRISK` can create risk score models that are sparser and more accurate when trained on a population from the same source as the test set.

Out-of-distribution Performance: We evaluate `GROUPFASTERRISK` models on the OOD dataset (see eICU Test Set in Figure 3b). We find that GFR-10 outperforms OASIS for both AUROC and AUPRC, with a noticeable margin of +0.039 and +0.075 for AUROC and AUPRC, respectively. Furthermore, GFR-15 achieves better predictive accuracy than SAPS II, with a margin of +0.015 for AUROC and +0.043 for AUPRC. We show the ROC and PR curves for eICU dataset in Figure 3a.

Although `GROUPFASTERRISK` is designed to optimize for sparse models, we include a more complex version, GFR-40, in our OOD evaluation for a thorough comparison with APACHE IV/IVa. We benchmark GFR-40 with APACHE IV/IVa on the eICU dataset. GFR-40 outperforms APACHE IV/IVa in terms of AUPRC with a margin of +0.008 for IV and +0.006 for IVa. Although APACHE IV/IVa has higher AUROC scores (+0.007 for IV and +0.009 for IVa), GFR-40 uses significantly less features (40 compared to 142 for APACHE IV/IVa). (In fact, APACHE cannot be calculated on the MIMIC III dataset at all, which is a disadvantage



(a) ROC (left) and PR (right) curves for predicting all-cause in-hospital mortality on OOD evaluation. Our GROUPFASTERRISK models achieve better performance than all scoring system baselines except for APACHE IV/IVa on ROC.

(b) GROUPFASTERRISK compare with the well-known severity of illness scores under different group sparsity constraints (equivalent to number of features). Evaluated on the internal MIMIC III dataset using 5-fold *nested* cross-validation, the best model from GROUPFASTERRISK is then evaluated in an OOD setting on the eICU cohort.

a. F is the number of features (equivalent to group sparsity) used by the model.

b. APACHE IV/IVa cannot be calculated on MIMIC III due to a lack of information for admission diagnoses.

		Sparse				Not Sparse		
		GFR-10 $F = 10$	OASIS $F = 10$	GFR-15 $F = 15$	SAPS II $F = 17$	GFR-40 $F = 40$	APACHE IV $F = 142$	APACHE IVa $F = 142$
MIMIC III	AUROC	0.813 ± 0.007	0.775 ± 0.008	0.836 ± 0.006	0.795 ± 0.009	0.858 ± 0.008		
Test Folds	AUPRC	0.368 ± 0.011	0.314 ± 0.014	0.403 ± 0.011	0.342 ± 0.012	0.443 ± 0.013		
	HL χ^2	16.28 ± 2.51	146.16 ± 10.27	26.73 ± 6.38	691.45 ± 18.64	35.78 ± 11.01		
	SMR	0.992 ± 0.022	0.686 ± 0.008	0.996 ± 0.015	0.485 ± 0.005	1.002 ± 0.017		
	Sparsity	42 ± 0	47	48 ± 4.9	58	66 ± 8.0		
eICU	AUROC	0.844	0.805	0.859	0.844	0.864	0.871	0.873
Test Set	AUPRC	0.437	0.361	0.476	0.433	0.495	0.487	0.489
	Sparsity	34	47	50	58	80	≥142	≥142

Figure 3: Comparison of GROUPFASTERRISK models with OASIS, SAPS II, APACHE IV, and APACHE IVa on all-cause in-hospital mortality prediction task.

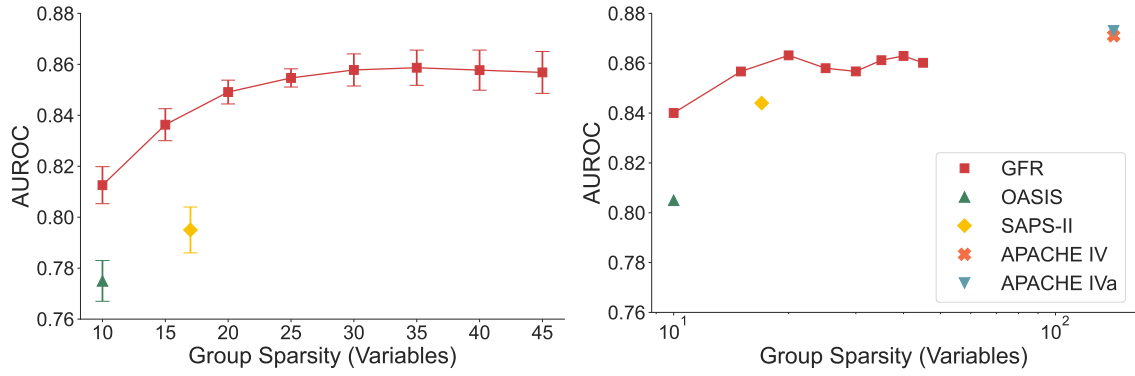
of complicated models in general.) Therefore, GROUPFASTERRISK can achieve comparable performance to sophisticated severity of illness scores while utilizing at least three times fewer parameters.

Group Sparsity and Runtime: Figure 4a shows the predictive accuracy of GROUPFASTERRISK models under different levels of group sparsity. We find that a higher group sparsity (equivalent to using more features) is positively correlated with an increase in predictive accuracy. However, the increase in AUROC becomes relatively small after 30 variables. It takes at most two hours to train GROUPFASTERRISK on our MIMIC III cohort (Figure 4b) (recall that MIMIC III cohort has 30,238 patients). This is a relatively short amount of time considering that GROUPFASTERRISK is solving a hard optimization problem, which is NP-hard and combinatorial in nature. We discuss more on our optimization techniques in Section 4.1.

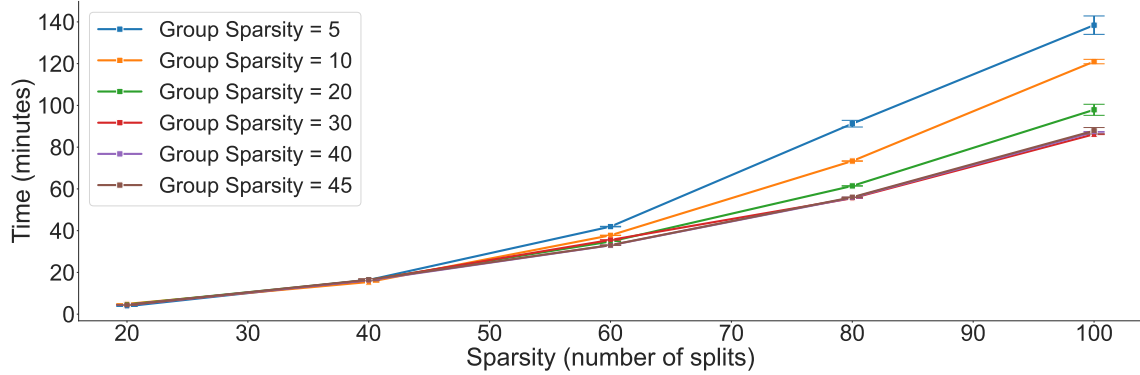
Overall, our results in Figure 3 suggest that GROUPFASTERRISK is capable of producing robust models that predict in-hospital mortality better or on par as compared to baseline scoring systems, while being more sparse on internal and OOD settings.

2.3 Critical Illness Mortality Prediction for Patients with Sepsis/Septicemia, Acute Kidney Failure, Acute Myocardial Infarction, and Heart Failure

For mortality prognosis tasks, patients with specific critical illnesses are often more prone to risk in ICU [8, 43, 45–49]. Thus, it is essential to evaluate whether GROUPFASTERRISK models can provide accurate risk prediction for those population sub-groups. To create disease-specific risk scores, we utilize International Classification of Diseases (ICD) codes in both MIMIC III and eICU to select patients with sepsis or septicemia, acute kidney failure, acute myocardial infarction, and heart failure for our study. We subsequently train GROUPFASTERRISK models on those sub-populations in the MIMIC III dataset. For simplicity, we refer to



(a) Performance of GROUPFASTERRISK under different levels of group sparsity. (Left) Internal evaluation on MIMIC III. (Right) OOD evaluation on eICU.



(b) Time consumption to train GROUPFASTERRISK under various sparsity and group sparsity constraints. Evaluated using five repeated trials on the entire MIMIC III dataset, with sample size of 30,238 and 49 features.

Figure 4: Group sparsities and time consumption of GROUPFASTERRISK.

patients in those four subgroups as *disease-specific* cohorts in the rest of this paper. Given that our selected critical illnesses are organ-failure-related, we incorporate SOFA [8] as an additional baseline. While SOFA was initially developed for assessing morbidity, subsequent studies have validated its utility in mortality prediction [50, 51], prompting our decision to include it for comparison.

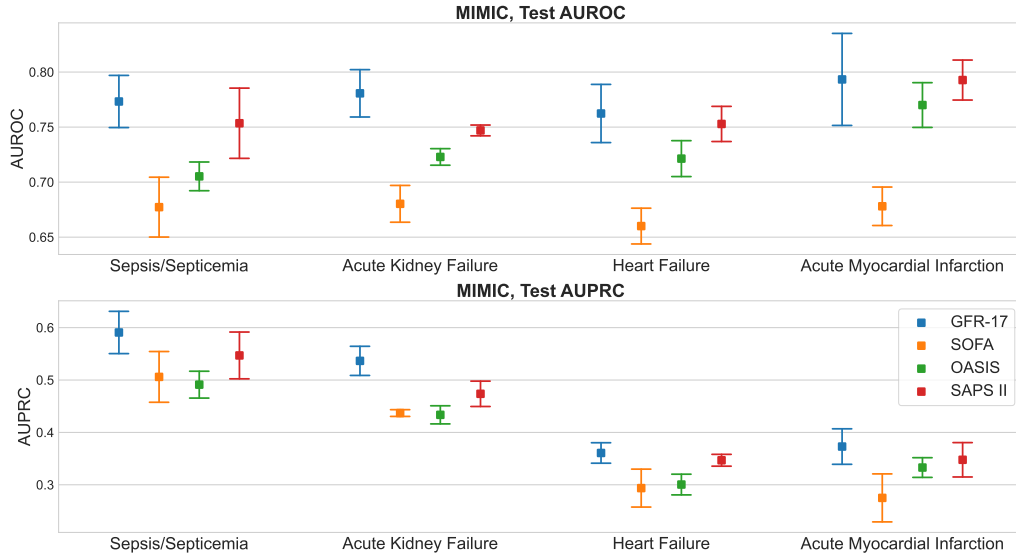
Figure 5a shows an evaluation across all four critical illnesses on internal MIMIC III test folds. GFR-17 achieves higher mean AUROC and AUPRC for all disease-specific cohorts when compared to OASIS, SOFA, and SAPS-II.

Figure 5b contains our results for OOD evaluation on eICU dataset. Here, we trained on the entire MIMIC III dataset, not on subgroups like we did for Figure 5a to be consistent with the other methods (that are used for all subgroups). Our GROUPFASTERRISK models outperform OASIS and SOFA across all disease-specific cohorts. GFR-40 models outperform APACHE IV/IVa for sepsis, septicemia, and acute kidney failure cohorts. For GFR-15, we observe higher predictive accuracy than SAPS II on both sepsis or septicemia and acute kidney failure cohorts.

Our results highlight the flexibility of GROUPFASTERRISK, as its models perform well across subgroups, and the method can also be tailored to subgroups if desired.

2.4 GROUPFASTERRISK Features Are More Informative Than OASIS Features

Since GROUPFASTERRISK is designed to find solutions for sparse logistic regression, we can alternatively use GROUPFASTERRISK as a tool for automated, data-driven feature selection. In particular, features selected by GROUPFASTERRISK should be more informative in predicting the outcome than those features that were not selected. Furthermore, the risk scores reveal how the risks change with each of the feature values.



(a) **Results in internal MIMIC III cohort.** (Top) performance evaluations based on AUROC. (Bottom) based on AUPRC. We show mean and standard deviation over five MIMIC III test folds. When compared to OASIS, GFR-17 has 0.068 higher mean AUROC for the sepsis or septicemia sub-group ($p < 0.05$), 0.058 higher mean AUROC for the acute kidney failure sub-group ($p < 0.05$), 0.041 higher mean AUROC for the heart failure sub-group ($p < 0.05$), and 0.023 higher mean AUROC for acute myocardial infarction sub-group ($p = 0.138$).

(b) **Results in OOD eICU cohort.** GROUPFASTERRISK is trained on the entire MIMIC III cohort (not on subgroups) using various group sparsity constraints. For each severity of illness score, our GROUPFASTERRISK models perform on par or better than its baseline while using fewer features.

		Sparse				Not Sparse			
		GFR-10 $F = 10$	OASIS $F = 10$	SOFA $F = 11$	GFR-15 $F = 15$	SAPS II $F = 17$	GFR-40 $F = 40$	APACHE IV $F = 142$	APACHE IVa $F = 142$
Sepsis/Septicemia	AUROC	0.776	0.734	0.726	0.783	0.782	0.794	0.780	0.781
	AUPRC	0.515	0.435	0.461	0.522	0.512	0.549	0.504	0.503
Acute Myocardial Infarction	AUROC	0.867	0.846	0.795	0.886	0.879	0.884	0.879	0.886
	AUPRC	0.455	0.424	0.395	0.486	0.493	0.521	0.493	0.498
Heart Failure	AUROC	0.755	0.731	0.702	0.766	0.770	0.785	0.782	0.787
	AUPRC	0.372	0.351	0.337	0.388	0.396	0.425	0.423	0.425
Acute Kidney Failure	AUROC	0.774	0.760	0.723	0.801	0.781	0.816	0.803	0.802
	AUPRC	0.514	0.472	0.462	0.550	0.527	0.583	0.552	0.550

Figure 5: Evaluation on disease-specific cohorts.

We now evaluate the ability of GROUPFASTERRISK to select good features on our internal MIMIC III dataset. To match the number of OASIS variables (see Methods section for details), we selected 14 distinct variables (including all of their thresholds) by training a GFR-14 model and extracting the fourteen features it chose. We then trained black box and interpretable ML models, including Logistic Regression, EBM, Random Forest, AdaBoost, and XGBoost, using features selected by GFR-14. To benchmark our results, we compare with the OASIS+ approach, which demonstrates that ML models trained on OASIS features can obtain high predictive accuracy [18]. Figure 6 shows a comparison of predictive accuracy between GFR-14 and OASIS features. We discover that the vast majority of ML models exhibit enhanced predictive performance when trained on GFR-14 features. More specifically, all models trained on GFR-14 features achieve statistically significantly higher AUROC and AUPRC than those trained on OASIS features ($p < 0.01$). Our results demonstrate that GROUPFASTERRISK naturally selects statistically useful features, enabling the development of ML models that are more predictive than the existing OASIS+ approach.

2.5 GROUPFASTERRISK Models Are Accurate and Sparse

As we observed in Figure 3 and Figure 5, GROUPFASTERRISK models outperform existing severity of illness scores in mortality prediction while being simpler. We further illustrate this point by comparing GROUP-

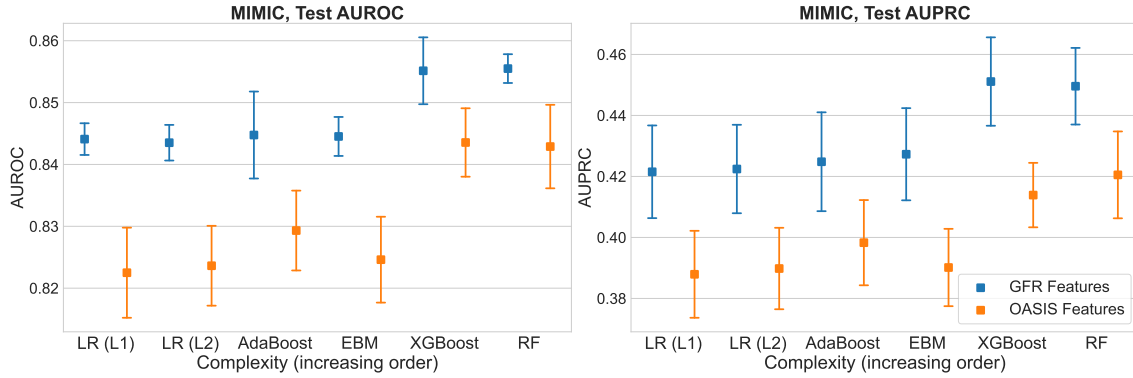


Figure 6: Predictiveness of GROUPFASTERRISK features against OASIS features. When evaluating the MIMIC III cohort, we find that GFR-14 features empower ML models to perform better than their counterparts when trained on OASIS features.

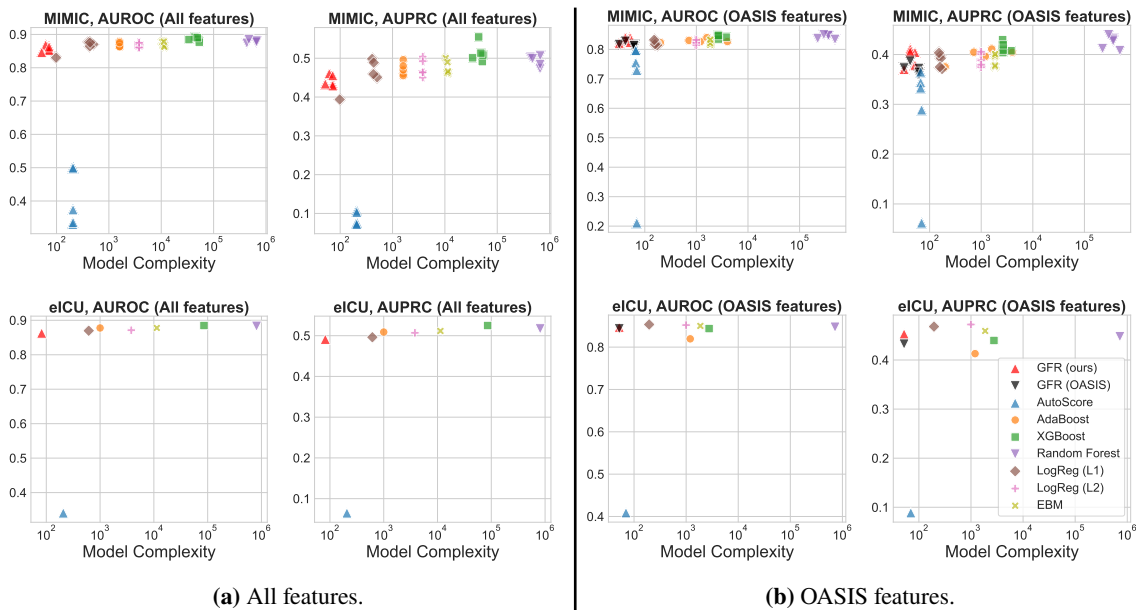


Figure 7: Performance vs. Complexity

FASTERRISK’s with more complex ML approaches. We will see that GROUPFASTERRISK is able to perform similarly to black box ML models while being orders of magnitude sparser.

We conduct two experiments to assess the relationship between our methods’ model complexity and AUROC or AUPRC. In the first experiment, we train different ML models using the OASIS features, including Logistic Regression, Random Forest, AdaBoost, EBM, XGBoost, and AutoScore. We compare their performance against our GFR-14 model (using our own features) and GROUPFASTERRISK trained on OASIS features, namely GFR-OASIS. In the second experiment, we train the same ML models using all 49 features we obtained from the MIMIC III dataset. We compare these models with GFR-40.

We show results based on OASIS features in Figure 7b and results based on all features in Figure 7a. For both setups, we find that GROUPFASTERRISK models (GFR-14, GFR-40, GFR-OASIS) consistently achieve the best sparsity and high AUROC and AUPRC. Among the different methods we compared with, AutoScore models are the least complex and rely on around 100 parameters, but their performance is substantially worse. Random Forest models achieve the highest AUROC and AUPRC scores, however, these models are very complex and rely on $\sim 10^6$ parameters, while GROUPFASTERRISK models use at most 82 parameters. Other methods such as ℓ_2 -regularized Logistic Regression and EBM were as complex as boosted decision

trees in terms of the total number of splits across all trees, $\sim 10^3$. To sum up, GROUPFASTERRISK models consistently have high performance while being orders of magnitude sparser than baseline models.

2.6 GROUPFASTERRISK Produces Reliable and Fair Risk Predictions

In critical care settings, the trustworthiness and fairness of a model’s predictions are paramount since they could considerably affect its usability [52]. To assess the GROUPFASTERRISK models and the severity of illness score baselines, we use the calibration and predictive accuracy metrics outlined in Section 2.1.1. We consider our eICU cohort for the evaluations because it offers a larger sample size and encompasses multi-center data from across the United States. Subsequently, we evaluate GROUPFASTERRISK models across various demographic subgroups, considering factors like ethnicity and gender.

Our results are presented in Table 1. We observe that GROUPFASTERRISK models are not particularly biased towards the majority race (Caucasians) and are well-calibrated on specific subgroups in our eICU cohort. GROUPFASTERRISK models consistently achieve low Brier scores and HL χ^2 across population subgroups. Except in a few cases, GROUPFASTERRISK models’ Brier scores, HL χ^2 , and SMR are better than those of OASIS, SAPS II, and APACHE IV/IVa. On average, across all ethnic and gender groups, GFR-10, GFR-15, and GFR-40 achieve SMR of 0.986 ± 0.041 , 1.004 ± 0.040 , and 1.005 ± 0.058 , respectively, which are all close to 1 (the best possible value). Among sparse models (no more than 17 variables), GROUPFASTERRISK achieves the highest AUROC and AUPRC across subgroups. We present additional ROC, PR, and calibration curves in Appendix C.3.

Table 1: Fairness and calibration across population subgroups in eICU.

		Ethnicity (alphabetical order)						Gender	
		African American	Asian	Caucasian	Hispanic	Native American	Other/Unknown	Female	Male
Percentage (%)		11.17	1.49	76.91	3.86	0.68	4.68	45.08	54.90
AUROC (\uparrow)	GFR-10	0.829	0.833	0.837	0.856	0.881	0.849	0.835	0.840
	OASIS	0.811	0.797	0.803	0.825	0.824	0.809	0.806	0.805
	GFR-15	0.846	0.848	0.854	0.873	0.895	0.860	0.853	0.856
	SAPS II	0.846	0.828	0.843	0.859	0.893	0.842	0.844	0.845
	GFR-40	0.859	0.861	0.859	0.881	0.902	0.873	0.857	0.865
	APACHE IV	0.873	0.858	0.869	0.890	0.903	0.884	0.867	0.875
	APACHE IVa	0.875	0.866	0.870	0.893	0.901	0.886	0.869	0.876
AUPRC (\uparrow)	GFR-10	0.415	0.390	0.422	0.480	0.558	0.418	0.418	0.429
	OASIS	0.345	0.330	0.364	0.410	0.370	0.328	0.356	0.365
	GFR-15	0.453	0.454	0.466	0.534	0.555	0.477	0.466	0.471
	SAPS II	0.424	0.408	0.435	0.470	0.598	0.395	0.440	0.428
	GFR-40	0.488	0.500	0.489	0.553	0.585	0.512	0.488	0.499
	APACHE IV	0.488	0.467	0.484	0.536	0.536	0.479	0.478	0.493
	APACHE IVa	0.487	0.492	0.487	0.538	0.522	0.484	0.481	0.496
Brier Score (\downarrow)	GFR-10	0.064	0.070	0.068	0.065	0.059	0.065	0.068	0.067
	OASIS	0.068	0.076	0.072	0.068	0.072	0.070	0.072	0.070
	GFR-15	0.062	0.068	0.065	0.061	0.059	0.061	0.065	0.064
	SAPS II	0.080	0.080	0.082	0.074	0.072	0.078	0.080	0.081
	GFR-40	0.060	0.064	0.064	0.060	0.057	0.059	0.064	0.062
	APACHE IV	0.063	0.069	0.066	0.062	0.066	0.064	0.066	0.064
	APACHE IVa	0.061	0.065	0.064	0.060	0.062	0.061	0.064	0.062
HL χ^2 (\downarrow)	GFR-10	27.90	11.00	113.70	24.68	5.48	12.53	58.65	102.74
	OASIS	43.48	21.02	135.52	5.23	14.84	11.75	82.52	79.11
	GFR-15	23.64	9.88	63.40	10.62	4.43	3.73	13.62	57.75
	SAPS II	1070.09	94.34	6599.71	228.75	62.95	333.65	3575.48	4750.90
	GFR-40	8.72	5.20	120.03	12.03	11.57	6.09	58.34	97.92
	APACHE IV	308.51	34.51	1257.11	78.93	42.53	114.22	835.14	950.18
	APACHE IVa	167.60	13.04	502.27	42.78	23.21	62.48	372.68	384.89
SMR (~ 1)	GFR-10	0.946	0.915	1.028	1.017	0.949	1.013	0.993	1.031
	OASIS	0.882	1.204	0.922	0.994	0.844	1.002	0.917	0.940
	GFR-15	0.974	0.921	1.040	1.046	1.003	0.996	1.002	1.046
	SAPS II	0.501	0.570	0.517	0.560	0.513	0.552	0.525	0.517
	GFR-40	1.022	0.936	1.039	1.063	0.889	1.033	1.000	1.058
	APACHE IV	0.663	0.732	0.731	0.710	0.606	0.697	0.716	0.725
	APACHE IVa	0.730	0.820	0.823	0.784	0.704	0.778	0.802	0.815

3 Discussion

Table 2: Comparison of GROUPFASTERRISK with other current mortality prediction methods.

*We consider the following Severity of Illness Scores: OASIS, SOFA, SAPS II, and APACHE IV/IVa

	GROUPFASTERRISK	Severity of Illness Scores*	Black-box ML	AutoScore
Interpretable models?	✓	✓	✗	✓
Can be trained on specific subpopulations?	✓	✗	✓	✓
Allow post-correction to suit domain knowledge.	✓	✗	✗	✓
Automatically produce risk cards?	✓	✗	✗	✓
Allow feature extraction?	✓	✓	✗	✓
Allow hard constraints in optimization?	✓	✗	✗	✓
High predictive accuracy?	✓	✓	✓	✗

Our work introduces GROUPFASTERRISK, an ML algorithm capable of creating a diverse set of accurate severity of illness scores while being highly flexible. We demonstrate that our approach generally outperforms existing severity of illness scores, is capable of selecting highly predictive variables, and performs well on population sub-groups based on race and gender in terms of robustness, accuracy, fairness, and calibration. Moreover, our models perform similarly to black-box ML models learned on the same data while being orders of magnitude sparser and simpler. Our framework provides an accessible and fast procedure to learn an interpretable model from data and could be used to support medical practitioners in the development of severity of illness scores and beyond. There are multiple aspects of our study worthy of discussion; we firstly focus on the advantages of GROUPFASTERRISK (summarized in Table 2) and then on the limitations of our study.

Interpretability: GROUPFASTERRISK generates scorecard displays (such as the one in Figure 1). From those displays, one can quickly evaluate the correctness of the model and make adjustments if desired. For instance, the feature component scores, shown as the rows in Figure 1, allow medical practitioners to interpret the relationship between risk (value of the integers) and the possible values of the features. Additionally, the group sparsity constraint γ enforces the selection of, at most, the top γ useful features, informing the user about the meaningful variables in the prediction-making process. Combined together, this score calculation process from GROUPFASTERRISK models is transparent and interpretable to the user at any level of medical expertise. This could be beneficial for healthcare applications in several ways: (1) It enables users to directly see the model itself and every single step of its prediction-making process, supporting the discovery of new knowledge or potential bias in the model without the need for post-hoc explanations. (2) If the model does not suit medical knowledge due to empirical noise in data, practitioners could further adopt monotonicity corrections to adjust the model. (3) The diverse pool of solutions provides users with a set of equally accurate risk scorecards, which helps to resolve the “interaction bottleneck” between people and algorithms. Users can choose among numerous available models to pick one that aligns the best with medical knowledge. These advantages can largely support health professionals in practice compared with black box ML models. (4) Our code includes the option of monotonicity constraints for interpretability. This allows, for instance, the user to constrain the risk scores to increase with age. To evaluate whether monotonicity correction can aid the development of more predictive models, we provide ablation studies in Appendix C.1. We find that models corrected with monotonicity constraints demonstrate increased predictive accuracy in OOD evaluations compared to the original, uncorrected models. This suggests that incorporating domain-relevant knowledge into risk score design could further enhance performance.

Sparsity: Among the different scoring systems we compared in the paper, APACHE IV/IVa is among the most accurate. Both APACHE IV/IVa rely on 142 features for a completed setup of patient risk predictions. In comparison, our most complex model GFR-40 achieves similar performances as APACHE IV/IVa while requiring only 40 features for its risk prediction process. In practice, this 3.5 times difference in the number of features can be quite significant, especially when accounted for missing values or other collection errors that commonly occur in medical data [53]. While there are several ways to handle missing data, such as treating missing values as 0 or using other statistical imputation techniques [54, 55], these methods can negatively affect prediction accuracy, limit performance guarantees, and create an extra task for medical practitioners to complete in practice. Since GFR-40 expects 40 features for its risk prognosis prediction, it is less likely to require practitioners to address missing value problems as compared to APACHE IV/IVa. Furthermore, compared to other ML approaches, GROUPFASTERRISK models are 1,000 times sparser in model

complexity while achieving comparable performance. Since studies have shown that humans can at most manage 7 ± 2 cognitive entities at the same time [56, 57], the sparse-learning nature of GROUPFASTERRISK can be supportive for medical practitioners since it is the basis for creating interpretable models.

Flexibility: Most existing severity of illness scores are fixed and provided as they are, making it difficult to adjust them to suit different populations. They are also not applicable to re-train and cannot be adapted for specific subpopulations. Moreover, they can be time- and resource- costly to construct and learn in the first place. For example, SAPS II was constructed from expert knowledge, and OASIS was created via a semi-manual process involving feature selection and fine-tuning of coefficients. By contrast, GROUPFASTERRISK is a data-driven ML algorithm capable of adapting to different datasets and producing risk scores tailored to any population in a reasonable amount of time. Rather than a fixed risk score, we provide a flexible system to compute *numerous* risk scores. Practitioners can set arbitrary grouping of the features, sparsity, and box constraints to design risk scores of their choice. They can learn a scoring system for a specific cohort of interest or different datasets. They can adjust risk scores manually if desired, using the approach of [58]. Further, as we discussed before, GROUPFASTERRISK can provide more than one high-performing solution as discussed in Figure 2. In this case, experts can choose a solution that they prefer and adopt a risk score that best suits their needs. GROUPFASTERRISK selects important features for prediction, which we have experimentally demonstrated in Figure 6. Lastly, although practitioners still need to determine GROUPFASTERRISK’s hyperparameters, they are fast to optimize. GROUPFASTERRISK is capable of creating risk scores within hours on a personal laptop (Apple MacBook Pro, M2).

Generalization: When models are applied across different high-risk settings, it is important that the model generalizes well. Our OOD evaluation is performed on the eICU, a dataset collected from other medical centers independent of our internal dataset MIMIC III. Therefore, we provide an estimate of generalization error by taking into consideration: (1) differences in practice between health systems, (2) variations in patient demographics, genotypes, and phenotypes, and (3) variations in hardware and software for data capture. All of these are important to the generalizability of models in healthcare systems [59]. Our OOD evaluation demonstrates that GROUPFASTERRISK can generalize well when trained on MIMIC III and tested on eICU for all-cause and disease-specific cohorts.

There are some limitations in how we evaluate the generalizability of GROUPFASTERRISK models. For instance, changes in patterns over time are still not fully measured. We discuss this issue in Limitation I and II.

Limitation I — Distributional Shifts: Due to data access issues, we could only conduct experiments on MIMIC III and eICU datasets and therefore, our results are limited to the setting of these study cohorts (however, as far as we are aware, these are the largest and most detailed publicly available datasets that have ever existed on ICU monitoring.). MIMIC III and eICU were collected between 2001-2012 and 2014-2015, respectively, which limits us from performing further evaluation on samples collected from the current period. For future research, it is worth investigating whether the results and conclusion still hold on samples from a different time period. Furthermore, changes in population distribution due to temporal drift have been shown to impact model predictive accuracy [60]. However, due to the de-identification process in both MIMIC III and eICU that keeps the admission date private, we are unable to perform such an evaluation. Second, both MIMIC III and eICU are datasets collected from hospitals in the United States. This limits the scope of our work in other countries, and thus our results may not be directly applicable to other geographical locations. Nonetheless, we believe further evaluations using data collected from different countries and a more recent time period could address these limitations. Our methods may be substantially faster in generating risk scores in different geographical areas and time periods than the considered baselines and competitors, since GROUPFASTERRISK constructs models automatically, rather than manually.

Limitation II — Data Collection Process: Given the retrospective nature of our study, there are inherent limitations related to how MIMIC III and eICU collect data, especially for time series measurements. For instance, vital signs in eICU are first recorded as one-minute averages and then stored as five-minute medians, implying our data may not perfectly represent true vital sign measurements in practice. Although our study does not involve the direct use of time series measurements in patient records, we use summary statistics that may still be affected by changes in measurement processing or aggregation.

Additionally, to have more access to the measurements of the patients, our MIMIC III cohort considers patients who stayed in the ICU for more than 24 hours (see Appendix A.1). Such design could cause bias in

our models in predicting mortality for patients admitted to the ICU for less than one day. Thus, to provide a more comprehensive evaluation, our eICU cohort relaxes this restriction by including all patients who have been admitted for more than 4 hours. This criteria is also more consistent with the study cohort used to create OASIS and APACHE IV and allows a more rigorous evaluation of GROUPFASTERRISK models. Our results in the previous section fully support that GROUPFASTERRISK performs well under these shifted hours of ICU stay.

Limitation III — APACHE IV/IVa in Internal Setting: Another limitation of our study is that we cannot compute APACHE IV/IVa scores on the MIMIC III dataset (due to the lack of information for admission diagnosis in MIMIC III). Again, APACHE IV/IVa requires 142 features, which provides a disadvantage to evaluation and practical use.

4 Methods

4.1 Finding High-quality Solutions with GROUPFASTERRISK

Define a dataset as $\mathcal{D} = \{1, \tilde{\mathbf{x}}_i, y_i\}_{i=1}^n$, where $y_i \in \{0, 1\}$ is a label, $\tilde{\mathbf{x}}_i \in \mathbb{R}^p$ is a binarized feature vector (see Section 4.3 for details), $\mathbf{x}_i \in \mathbb{R}^q$ is the raw feature vector, and 1 is added for ease of notation and represents an intercept. The set of feature indices $\{1, \dots, p\}$ is arbitrarily partitioned into Γ disjoint sets (groups), denoted as $\{G_k\}_{k=1}^\Gamma$. Let $\mathcal{D}/m = \{1/m, \tilde{\mathbf{x}}_i/m, y_i\}_{i=1}^n$ be a scaled dataset, where we scale by a multiplier m , $m > 0$ (m will be learned by the algorithm). Let our hypothesis space be a space of linear models $\mathbf{w}^\top \tilde{\mathbf{x}} + w_0$, where $\mathbf{w} \in \mathbb{R}^p$ and $w_0 \in \mathbb{R}$. We denote $\mathbf{w}_{G_k} \in \mathbb{Z}^{|G_k|}$ as entries in \mathbf{w} that belong to a group G_k .

Our goal is to obtain *integer-valued* solutions of a *sparse* (ℓ_0 regularized) logistic regression problem under sparsity, group sparsity, and box constraints, denoted as λ , γ , (\mathbf{a}, \mathbf{b}) , respectively, where $\mathbf{a}, \mathbf{b} \in \mathbb{R}^p$, $w_j \in [a_j, b_j]$ for all j . We denote a solution as (\mathbf{w}, w_0) and outline the purpose of each hyperparameter below.

Sparsity: The sparsity constraint λ is the number of non-zero elements in the solution vector \mathbf{w} and directly controls the model complexity in the risk scorecards. The users can directly set λ , and GROUPFASTERRISK produces a diverse pool of solutions that strictly satisfies this hard constraint. Intuitively, when GROUPFASTERRISK is trained on binarized data, λ corresponds to the number of binary stumps or decision splits in the final model(s).

Group Sparsity: Group sparsity constraint γ allows users to control the number of partitions on the features in the final solution. In most cases and throughout all our experiments, binary stumps belonging to a single feature could be treated as a group. Under this treatment of groups, using group sparsity of γ is equivalent to optimizing the risk score using at most γ features, allowing the creation of more cohesive models for users to interpret. Alternatively, medical practitioners could also define groups based on similarity between features using their domain knowledge, such as grouping height and weight together since they are both biometric attributes, creating risk scores that best suit their needs.

Box Constraint: Box constraint (\mathbf{a}, \mathbf{b}) is also defined by the user and allows users to limit the solution values to their desired range, i.e., $w_j \in [a_j, b_j]$. This hyperparameter allows users to control the range of the coefficients on their final risk scores, providing more control over the final solution(s).

Overall, the problem of computing an integer-valued linear model is NP-hard. However, we solved it by finding a good approximate solution and using m as a multiplier to do so. While (\mathbf{w}, w_0) must be integer-valued, the product $(\mathbf{w}^\top \tilde{\mathbf{x}}/m + w_0/m)$ can be real-valued. Intuitively, division by a range of multipliers extends through the solution space like the rays of a star, and a subroutine is adopted to determine the multiplier.

We formulate the problem of creating risk scores as an optimization problem in Equation (1). More specifically, we optimize logistic loss in Equation (1a) for real-valued solution $(\mathbf{w}^\top \tilde{\mathbf{x}}/m + w_0/m)$, with sparsity constraint λ and integer constraint (Equation (1b)), box constraint (\mathbf{a}, \mathbf{b}) (Equation (1c)), group sparsity constraint γ (Equation (1e)), and multiplier m (Equation (1d)), where $\mathbb{I}\{\cdot\}$ denotes the indicator function.

$$\min_{\mathbf{w}, w_0, m} \mathcal{L}(\mathbf{w}, w_0, \mathcal{D}/m) = \sum_{i=1}^n \log \left(1 + \exp \left(-y_i \frac{\mathbf{w}^\top \tilde{\mathbf{x}}_i + w_0}{m} \right) \right) \quad (1a)$$

$$\text{s.t. } \|\mathbf{w}\|_0 \leq \lambda, \mathbf{w} \in \mathbb{Z}^p, w_0 \in \mathbb{Z} \quad \# \text{ at most } \lambda \text{ integer coefficients} \quad (1b)$$

$$w_j \in [a_j, b_j] \quad \forall j \in \{1, \dots, p\} \quad \# \text{ control range of coefficients} \quad (1c)$$

$$m > 0 \quad \# \text{ expand solution space using multiplier} \quad (1d)$$

$$\sum_{k=1}^{\Gamma} \mathbb{I}\{\mathbf{w}_{G_k} \neq \mathbf{0}\} \leq \gamma. \quad \# \text{ at most } \gamma \text{ groups, where } G_k \text{ are the indices of group } k \quad (1e)$$

We solve the optimization problem in Equation (1) similarly to [29] in three steps (as in Figure 2):

1. We first relax the integer value constraints and find a real-valued solution $(\mathbf{w}^{(*)}, w_0^{(*)})$ to sparse logistic regression under box constraint (\mathbf{a}, \mathbf{b}) .
2. Based on $(\mathbf{w}^{(*)}, w_0^{(*)})$, we swap one feature at a time to obtain a set of M sparse diverse real-valued solutions. We use an iterative subroutine to select the features, each of which must strictly satisfy the group constraint γ . We call this set Diverse Pool and denote the set by $\{(\mathbf{w}^{(t)}, w_0^{(t)})\}_{t=1}^M$. Diverse Pool's solutions are nearly as accurate as our original solution $(\mathbf{w}^{(*)}, w_0^{(*)})$.
3. For every solution in the Diverse Pool $\{(\mathbf{w}^{(t)}, w_0^{(t)})\}_{t=1}^M$, we round all the continuous solutions to integers, thus assigning weights to the selected variables and producing a set of risk scores. Unlike direct rounding that could worsen solution quality, we specifically use a subroutine that adapts multiplier m to extend the solution space when rounding the coefficients. A theoretical upper bound on the rounding error is proven in [29]; this choice permits us to maintain a high level of accuracy while rounding.

Together, the three steps allow GROUPFASTERRISK to produce multiple diverse sparse risk scores with high accuracy. Finally, for a given solution (\mathbf{w}, w_0) , we compute risk predictions as $P(Y = 1 | \tilde{\mathbf{x}}) = \sigma((\mathbf{w}^\top \tilde{\mathbf{x}} + w_0) / m)$, where $\sigma(\xi) = 1 / (1 + e^{-\xi})$ is a sigmoid function.

4.2 Feature Selection and Engineering

Our feature selection process was divided into two stages. First, we created a set of features by taking the union of features used by existing severity of illness scores. Specifically, we consider features from Acute Physiology Score III (APS III) [61], Simplified Acute Physiology Score II (SAPS II) [42], Oxford Acute Severity of Illness Score (OASIS) [14], Sequential Organ Failure Assessment (SOFA) [8], Logistic Organ Dysfunction Score (LODS) [62], and Systemic Inflammatory Response Syndrome criteria (SIRS) [63]. Second, we computed the receiver operating characteristic curve (ROC) and the corresponding area under the curve (AUC) value for every feature individually. By analyzing AUC and the shape of ROC curves, we estimate the predictive ability of every feature on in-hospital mortality for all the patients in the MIMIC III training set. This provides us with a ranking of all features, and we selected the top 49 features for this study.

To include time series measurements such as vital signs, we extracted the minimum and maximum of these features during the first 24 hours of a patient's unit stay. This allows us to focus on the worst deviation from a normal range of values. Minimum and maximum values of time series data are often easier to observe by medical practitioners than other more sophisticated statistics (such as variance), making them convenient from a practical point of view. Additionally, most existing severity of illness scores also rely on the worst values over a time period.

4.3 Feature Binarization

We transformed every continuous or categorical feature into a set of binary decision splits. This allows GROUPFASTERRISK to capture a non-linear step function for each feature when it learns coefficients for those decision splits. For continuous variables, a step function on feature l at threshold $\theta_{l,\bar{i}}$ would be denoted $\mathbb{I}\{x_l \leq \theta_{l,\bar{i}}\}$, which is 1 if $x_l \leq \theta_{l,\bar{i}}$ and 0 otherwise. The component function for feature l would then sum up the step functions for all the thresholds and would be denoted $f_l(x_l) = \sum_{\bar{i} \in G_l} w_{\bar{i}} \mathbb{I}\{x_l \leq \theta_{l,\bar{i}}\}$. The full model $f(\mathbf{x})$ would be the sum of the component functions, $\sum_l f_l(x_l)$. We used two methods to create the splits $\theta_{l,\bar{i}}$: 1) For binary or categorical features, a split was created between each pair of unique feature values for each feature. 2) We obtained the distribution of feature values based on the training data and

computed quantiles of the distributions and used them as decision splits. (Alternatively, the splits can be set as a hyperparameter.) This preprocessing procedure makes GROUPFASTERRISK models generalized additive models (GAMs), which have been demonstrated to be as accurate as any black box ML model for most tabular data problems [33, 64, 65].

4.4 GROUPFASTERRISK Monotonic Correction

GROUPFASTERRISK provides the option of a monotonic correction so that the risk score is forced to increase (or decrease) along a variable. This allows users to better align the modeling process with domain knowledge. More specifically, GROUPFASTERRISK allows users to set box constraints $(\mathbf{a}_{G_l}, \mathbf{b}_{G_l})$ for each feature l independently (recall that we set each group as the decision splits belonging to each feature). These constraints can be imposed after any of the three GROUPFASTERRISK optimization steps. Because of the binarization preprocessing step, each feature corresponds to a set of step functions. Imposing monotonicity is equivalent to forcing all coefficients for all step functions of one feature to be positive (for decreasing functions) or negative (for increasing functions). If $\mathbf{a}_{G_l}, \mathbf{b}_{G_l} \geq \mathbf{0}$, then $f_l(x_l)$ is monotonically decreasing; if $\mathbf{a}_{G_l}, \mathbf{b}_{G_l} \leq \mathbf{0}$, then component function f_l is monotonically increasing.

Our risk score in Figure 1 has been applied with monotonicity correction. Particularly, we set the box constraint for *Max Bilirubin* and *Max BUN* to be between $[-100, 0]$ and *Min GCS* and *Min SBP* to be between $[0, 100]$. This helps to prevent the algorithm from overfitting the model to noise in the data. For instance, without monotonicity constraints, we observed that the component function for *Min GCS* was non-monotonic at extreme values. This model would imply that patients with GCS of 3 are less risky than those with GCS of 6, which (while a realistic reflection of the information contained in the training data) is not aligned with medical knowledge. Our monotonicity correction prevents this from happening.

4.5 Training and Evaluation of GROUPFASTERRISK and ML Baselines

We trained GROUPFASTERRISK models with various group sparsity constraints between 10 and 45. For each group sparsity, we performed hyperparameter optimization using grid search and Bayesian optimization to determine the optimal hyperparameter. We ran two sets of experiments to evaluate GROUPFASTERRISK.

First, we used 5-fold *nested* cross-validation to evaluate performance on MIMIC III, i.e., we performed hyperparameter optimization on the training fold for each train/test split and used the best hyperparameter on the test set for evaluation.

Our second set of experiments evaluates the performance out of sample on the eICU dataset. We trained our models and performed hyperparameter optimization on the MIMIC III dataset, and evaluated them on the eICU cohort.

We used the same training and evaluation procedures for the ML baselines. The hyperparameters used in this study are contained in our code repository.

4.6 Severity of Illness Scores Evaluation

We benchmarked the performance of GROUPFASTERRISK against established severity of illness scores on MIMIC III and eICU study cohorts. For MIMIC III, we implemented the risk score calculation made by MIT-LCP. In particular, we calculated OASIS, SOFA, and SAPS-II for in-hospital mortality risk prediction and evaluated their performance on the same 5 test folds as GROUPFASTERRISK. We also attempted to calculate APACHE IV/IVa score on MIMIC III, but we ran into difficulty because the reason of admission variable was difficult to obtain. Although such information could potentially be inferred using natural language processing on the *Noteevents* table [30], this inference procedure has not been verified to reliably extract factually correct information, so we did not compute APACHE IV/IVa on MIMIC III.

For OOD evaluation on eICU, we referenced the OASIS calculation using the official code repository and calculated SAPS-II and SOFA scores from their published formulas. APACHE IV/IVa in-hospital mortality predictions are directly contained within the eICU dataset. We evaluated all severity of illness score baselines on the same study cohort as GROUPFASTERRISK.

4.7 Fairness and Calibration Evaluations

We used the eICU dataset for fairness evaluation since it has a multi-center data source collected from the entire United States. It has the advantage of containing more samples for each subgroup than MIMIC III. We separated the subgroups from the eICU study cohort by race and gender. For GROUPFASTERRISK, AUROC and AUPRC were computed for each subgroup using models trained on the entire MIMIC III cohort. In other words, GROUPFASTERRISK models were trained on the entire training population, without fitting to specific populations, and evaluated on the subgroups in the OOD setting. For severity of illness score baselines, we calculated AUROC and AUPRC directly on every eICU subgroup.

We calibrated GROUPFASTERRISK using *isotonic regression* on a subset of 2,000 patients drawn randomly from our eICU cohort, equivalent to about 1.84% of the entire cohort. We also provided the comparative experiment where we calibrate severity of illness score baselines in Appendix C.3; the results did not change.

5 Data Availability

Medical Information Mart for Intensive Care III Database (MIMIC-III) and eICU Collaborative Research Database (eICU or eICU-CRD)[30, 31] are both publicly available at <https://mimic.mit.edu/> and <https://eicu-crd.mit.edu/>, respectively. Access to the datasets require CITI Data or Specimens Only Research certifications and signing corresponding data use agreements, as well as institutional IRB approval at Duke.

6 Code Availability

The software developed in this study is available at <https://github.com/jiachangliu/FasterRisk>. The source code for experiments involved in this study is available at <https://github.com/MuhangTian/GFR-Experiments>.

References

1. McNamara, R. L. *et al.* Predicting in-hospital mortality in patients with acute myocardial infarction. *Journal of the American College of Cardiology* **68**, 626–635 (2016).
2. Edwards, F. H. *et al.* Development and validation of a risk prediction model for in-hospital mortality after transcatheter aortic valve replacement. *JAMA Cardiology* **1**, 46–52 (2016).
3. Fonarow, G. C. *et al.* Risk stratification for in-hospital mortality in acutely decompensated heart failure: classification and regression tree analysis. *JAMA* **293**, 572–580 (2005).
4. Barriere, S. L. & Lowry, S. F. An overview of mortality risk prediction in sepsis. *Critical Care Medicine* **23**, 376–393 (1995).
5. El-Solh, A. A., Lawson, Y., Carter, M., El-Solh, D. A. & Mergenhagen, K. A. Comparison of in-hospital mortality risk prediction models from COVID-19. *PLoS One* **15**, e0244629 (2020).
6. Kar, S. *et al.* Multivariable mortality risk prediction using machine learning for COVID-19 patients at admission (AICOVID). *Scientific Reports* **11**, 12801 (2021).
7. Knaus, W. A., Zimmerman, J. E., Wagner, D. P., Draper, E. A. & Lawrence, D. E. APACHE—acute physiology and chronic health evaluation: a physiologically based classification system. *Critical Care Medicine* **9**, 591–597 (1981).
8. Vincent, J. *et al.* The SOFA (Sepsis-related Organ Failure Assessment) score to describe organ dysfunction/failure: On behalf of the Working Group on Sepsis-Related Problems of the European Society of Intensive Care Medicine (see contributors to the project in the appendix) 1996.
9. Singer, M. *et al.* The third international consensus definitions for sepsis and septic shock (Sepsis-3). *JAMA* **315**, 801–810 (2016).
10. Knaus, W. A., Draper, E. A., Wagner, D. P. & Zimmerman, J. E. APACHE II: a severity of disease classification system. *Critical Care Medicine* **13**, 818–829 (1985).
11. Le Gall, J.-R. *et al.* A simplified acute physiology score for ICU patients. *Critical Care Medicine* **12**, 975–977 (1984).
12. Zimmerman, J. E., Kramer, A. A., McNair, D. S. & Malila, F. M. Acute Physiology and Chronic Health Evaluation (APACHE) IV: hospital mortality assessment for today’s critically ill patients. *Critical Care Medicine* **34**, 1297–1310 (2006).

13. Cleveland, W. S. Robust locally weighted regression and smoothing scatterplots. *Journal of the American Statistical Association* **74**, 829–836 (1979).
14. Johnson, A. E., Kramer, A. A. & Clifford, G. D. A new severity of illness scale using a subset of acute physiology and chronic health evaluation data elements shows comparable predictive accuracy. *Critical Care Medicine* **41**, 1711–1718 (2013).
15. Katoch, S., Chauhan, S. S. & Kumar, V. A review on genetic algorithm: past, present, and future. *Multimedia Tools and Applications* **80**, 8091–8126 (2021).
16. Kennedy, J. & Eberhart, R. *Particle swarm optimization* in *Proceedings of ICNN'95-International Conference on Neural Networks* **4** (1995), 1942–1948.
17. Choi, M. H. *et al.* Mortality prediction of patients in intensive care units using machine learning algorithms based on electronic health records. *Scientific Reports* **12**, 7180 (2022).
18. El-Manzalawy, Y. *et al.* OASIS+: leveraging machine learning to improve the prognostic accuracy of OASIS severity score for predicting in-hospital mortality. *BMC Medical Informatics and Decision Making* **21**, 156 (2021).
19. Levin, S. *et al.* Machine-learning-based electronic triage more accurately differentiates patients with respect to clinical outcomes compared with the emergency severity index. *Annals of Emergency Medicine* **71**, 565–574 (2018).
20. Klug, M. *et al.* A gradient boosting machine learning model for predicting early mortality in the emergency department triage: devising a nine-point triage score. *Journal of General Internal Medicine* **35**, 220–227 (2020).
21. Hong, W. S., Haimovich, A. D. & Taylor, R. A. Predicting hospital admission at emergency department triage using machine learning. *PloS One* **13**, e0201016 (2018).
22. González-Nóvoa, J. A. *et al.* Using explainable machine learning to improve intensive care unit alarm systems. *Sensors* **21**, 7125 (2021).
23. Breiman, L. Random forests. *Machine Learning* **45**, 5–32 (2001).
24. Chen, T. *et al.* Xgboost: extreme gradient boosting. *R package version 0.4-2* **1**, 1–4 (2015).
25. Rudin, C. Stop explaining black box machine learning models for high stakes decisions and use interpretable models instead. *Nature Machine Intelligence* **1**, 206–215 (2019).
26. Xie, F., Chakraborty, B., Ong, M. E. H., Goldstein, B. A., Liu, N., *et al.* AutoScore: a machine learning-based automatic clinical score generator and its application to mortality prediction using electronic health records. *JMIR Medical Informatics* **8**, e21798 (2020).
27. Ustun, B. & Rudin, C. *Optimized risk scores* in *Proceedings of the 23rd ACM SIGKDD international conference on knowledge discovery and data mining* (2017), 1125–1134.
28. Ustun, B. & Rudin, C. Learning Optimized Risk Scores. *J. Mach. Learn. Res.* **20**, 1–75 (2019).
29. Liu, J., Zhong, C., Li, B., Seltzer, M. & Rudin, C. *FasterRisk: Fast and Accurate Interpretable Risk Scores* in *Advances in Neural Information Processing Systems* **35** (Curran Associates, Inc., 2022), 17760–17773.
30. Johnson, A. E. *et al.* MIMIC-III, a freely accessible critical care database. *Scientific Data* **3**, 1–9 (2016).
31. Pollard, T. J. *et al.* The eICU Collaborative Research Database, a freely available multi-center database for critical care research. *Scientific Data* **5**, 1–13 (2018).
32. Davis, J. & Goadrich, M. *The relationship between Precision-Recall and ROC curves* in *Proceedings of the 23rd International Conference on Machine Learning* (2006), 233–240.
33. Lou, Y., Caruana, R. & Gehrke, J. *Intelligible models for classification and regression* in *Proceedings of the 18th ACM SIGKDD International Conference on Knowledge Discovery and Data Mining* (2012), 150–158.
34. Chen, T. & Guestrin, C. *Xgboost: A scalable tree boosting system* in *Proceedings of the 22nd ACM SIGKDD International Conference on Knowledge Discovery and Data Mining* (2016), 785–794.
35. Freund, Y. & Schapire, R. E. A decision-theoretic generalization of on-line learning and an application to boosting. *Journal of Computer and System Sciences* **55**, 119–139 (1997).
36. Huang, Y., Li, W., Macheret, F., Gabriel, R. A. & Ohno-Machado, L. A tutorial on calibration measurements and calibration models for clinical prediction models. *Journal of the American Medical Informatics Association* **27**, 621–633 (2020).
37. Brier, G. W. Verification of forecasts expressed in terms of probability. *Monthly Weather Review* **78**, 1–3 (1950).

38. Lemeshow, S. & Hosmer Jr, D. W. A review of goodness of fit statistics for use in the development of logistic regression models. *American Journal of Epidemiology* **115**, 92–106 (1982).
39. Rudin, C. *et al.* Interpretable machine learning: Fundamental principles and 10 grand challenges. *Statistic Surveys* **16**, 1–85 (2022).
40. Fisher, A., Rudin, C. & Dominici, F. All Models are Wrong, but Many are Useful: Learning a Variable’s Importance by Studying an Entire Class of Prediction Models Simultaneously. *Journal of Machine Learning Research* **20**, 1–81 (2019).
41. Semenova, L., Rudin, C. & Parr, R. *On the existence of simpler machine learning models* in *Proceedings of the 2022 ACM Conference on Fairness, Accountability, and Transparency* (2022), 1827–1858.
42. Le Gall, J.-R., Lemeshow, S. & Saulnier, F. A new simplified acute physiology score (SAPS II) based on a European/North American multicenter study. *JAMA* **270**, 2957–2963 (1993).
43. Seymour, C. W. *et al.* Assessment of clinical criteria for sepsis: for the Third International Consensus Definitions for Sepsis and Septic Shock (Sepsis-3). *JAMA* **315**, 762–774 (2016).
44. Lou, Y., Caruana, R., Gehrke, J. & Hooker, G. *Accurate intelligible models with pairwise interactions* in *Proceedings of the 19th ACM SIGKDD International Conference on Knowledge Discovery and Data Mining* (2013), 623–631.
45. Chen, Y.-C. *et al.* Risk factors for ICU mortality in critically ill patients. *Journal of the Formosan Medical Association* **100**, 656–661 (2001).
46. Angus, D. C. *et al.* Epidemiology of severe sepsis in the United States: analysis of incidence, outcome, and associated costs of care. *Critical Care Medicine* **29**, 1303–1310 (2001).
47. Members, W. G. *et al.* Heart disease and stroke statistics—2012 update: a report from the American Heart Association. *Circulation* **125**, e2–e220 (2012).
48. Marshall, J. C. *et al.* Multiple organ dysfunction score: a reliable descriptor of a complex clinical outcome. *Critical Care Medicine* **23**, 1638–1652 (1995).
49. Bellomo, R., Ronco, C., Kellum, J. A., Mehta, R. L. & Palevsky, P. Acute renal failure—definition, outcome measures, animal models, fluid therapy and information technology needs: the Second International Consensus Conference of the Acute Dialysis Quality Initiative (ADQI) Group. *Critical Care* **8**, 1–9 (2004).
50. Minne, L., Abu-Hanna, A. & de Jonge, E. Evaluation of SOFA-based models for predicting mortality in the ICU: A systematic review. *Critical Care* **12**, 1–13 (2008).
51. Fayed, M. *et al.* Sequential organ failure assessment (SOFA) score and mortality prediction in patients with severe respiratory distress secondary to COVID-19. *Cureus* **14** (2022).
52. Mehrabi, N., Morstatter, F., Saxena, N., Lerman, K. & Galstyan, A. A survey on bias and fairness in machine learning. *ACM Computing Surveys (CSUR)* **54**, 1–35 (2021).
53. Zhou, Y. *et al.* Missing data matter: an empirical evaluation of the impacts of missing EHR data in comparative effectiveness research. *Journal of the American Medical Informatics Association*, ocad066 (2023).
54. Van Buuren, S. & Groothuis-Oudshoorn, K. mice: Multivariate imputation by chained equations in R. *Journal of Statistical Software* **45**, 1–67 (2011).
55. Lin, W.-C. & Tsai, C.-F. Missing value imputation: a review and analysis of the literature (2006–2017). *Artificial Intelligence Review* **53**, 1487–1509 (2020).
56. Miller, G. A. The magical number seven, plus or minus two: Some limits on our capacity for processing information. *Psychological Review* **63**, 81 (1956).
57. Cowan, N. The magical mystery four: How is working memory capacity limited, and why? *Current Directions in Psychological Science* **19**, 51–57 (2010).
58. Wang, Z. J. *et al.* Interpretability, then what? editing machine learning models to reflect human knowledge and values in *Proceedings of the 28th ACM SIGKDD Conference on Knowledge Discovery and Data Mining* (2022), 4132–4142.
59. Futoma, J., Simons, M., Panch, T., Doshi-Velez, F. & Celi, L. A. The myth of generalisability in clinical research and machine learning in health care. *The Lancet Digital Health* **2**, e489–e492 (2020).
60. Nestor, B. *et al.* Feature robustness in non-stationary health records: caveats to deployable model performance in common clinical machine learning tasks in *Machine Learning for Healthcare Conference* (2019), 381–405.
61. Knaus, W. A. *et al.* The APACHE III prognostic system: risk prediction of hospital mortality for critically III hospitalized adults. *Chest* **100**, 1619–1636 (1991).

62. Le Gall, J.-R. *et al.* The Logistic Organ Dysfunction system: a new way to assess organ dysfunction in the intensive care unit. *JAMA* **276**, 802–810 (1996).
63. Bone, R. C. *et al.* Definitions for sepsis and organ failure and guidelines for the use of innovative therapies in sepsis. *Chest* **101**, 1644–1655 (1992).
64. Hastie, T. J. & Tibshirani, R. J. *Generalized additive models* (CRC press, 1990).
65. Wang, C., Han, B., Patel, B. & Rudin, C. In pursuit of interpretable, fair and accurate machine learning for criminal recidivism prediction. *Journal of Quantitative Criminology*, 1–63 (2022).

Appendix to “Fast and Interpretable Mortality Risk Scores for Critical Care Patients”

Table of Contents

A Experiment Details	21
A.1 Study Population	21
A.2 Severity of Illness Score Implementations	21
B GROUPFASTERRISK Algorithm	23
B.1 Optimization Procedures Outline	23
C Additional Experiments	24
C.1 Source of Gains for Risk Score Generation	24
C.2 Performance Comparisons	24
C.3 Fairness and Calibration Evaluations	27
C.4 GROUPFASTERRISK Performances	29
C.5 Visualizations of Risk Scores Generated by GROUPFASTERRISK	29

A Experiment Details

A.1 Study Population

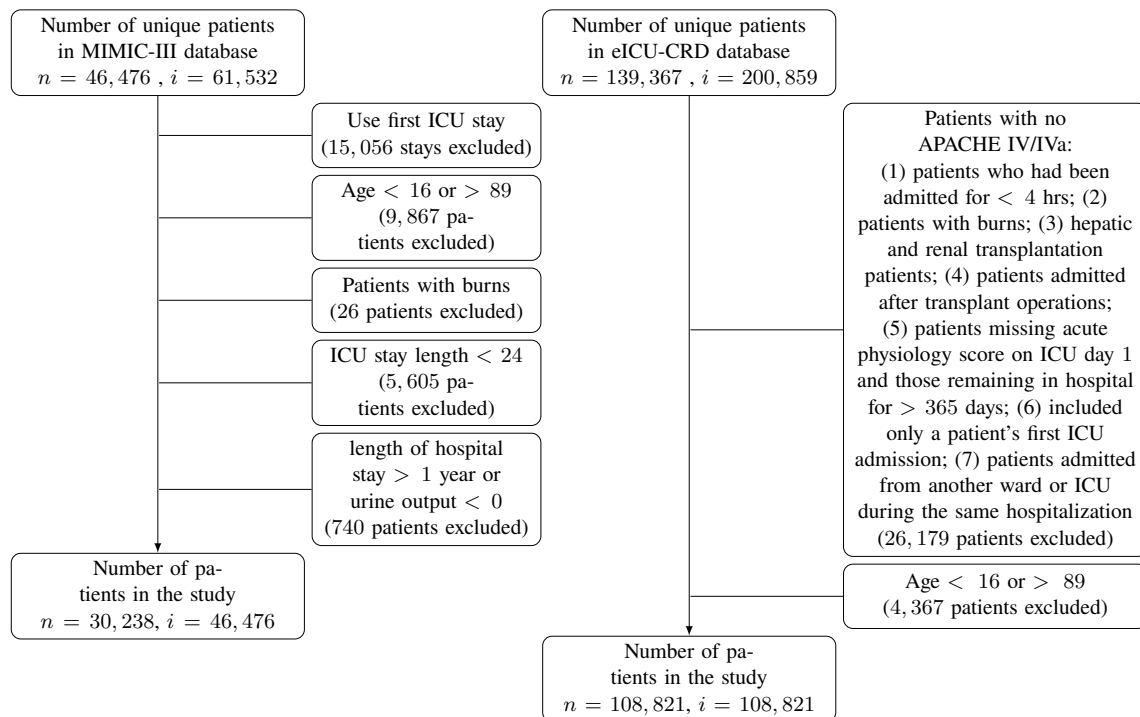


Figure 8: Flow chart of the study population selection on MIMIC III and eICU-CRD database. i and n are ICU stays and number of patients, respectively.

MIMIC-III

MIMIC-III is a large, single-center database comprised of health-related information of 53,423 hospital admissions for adult patients (aged 16 years or above) admitted to critical care units of the Beth Israel Deaconess Medical Center in Boston, MA, between 2001 and 2012. MIMIC-III integrates de-identified, comprehensive clinical data of 38,597 distinct adult patients. It includes patient information such as laboratory measurements, vital signs, notes charted by healthcare providers, diagnostic codes, hospital length of stay, and survival data. Besides mortality prediction, MIMIC-III has been used by academic and industrial research to investigate novel clinical relationships and develop new algorithms for patient monitoring [30].

eICU

The eICU Collaborative Research Database, sourced from the eICU Telehealth Program, is a multi-center ICU database with high granularity data containing 200,859 admissions to ICUs monitored by eICU programs across the United States. The database includes 139,367 unique patients admitted to critical care units in 2014 and 2015. Built upon the success of MIMIC-III, eICU includes patients from multiple medical centers. The source hospital of MIMIC-III does not participate in the eICU program, which makes eICU a completely independent set of healthcare data suitable for out-of-distribution evaluation [31].

A.2 Severity of Illness Score Implementations

We observe a discrepancy between official implementations of OASIS and SAPS II in the MIMIC III code repository with their respective original works. In particular, the calculation of the sub-score for pre-ICU length of stay differs from that published in the original paper [14], and the implementation for bicarbonate sub-score in SAPS II also differs from the original work in [42]. Details of the implementation errors can

be found in [this GitHub issue](#). We corrected those mistakes in our implementations for OASIS and SAPS II and detailed the effects caused by our corrections in Table 3.

The APACHE IV/IVa scores are directly contained in the eICU dataset [31], thus, there was no need to implement these scores ourselves.

Table 3: Effect of implementation correction for OASIS and SAPS II.

		OASIS Correction	SAPS II Correction
MIMIC III	Affected Patients (%) ^a	22.93	4.38
	AUROC Change	+0.001	0.000
	AUPRC Change	-0.001	+0.001
	HL χ^2 Change	+18.59	+17.06
	Brier Score Change	+0.001	0.000
	SMR Change	-0.011	-0.002
eICU	Affected Patients (%)	14.07	6.09
	AUROC Change	+0.002	0.000
	AUPRC Change	+0.001	+0.001
	HL χ^2 Change	+13.77	+206.87
	Brier Score Change	0.000	0.000
	SMR Change	-0.012	-0.002

B GROUPFASTERRISK Algorithm

B.1 Optimization Procedures Outline

We use the same notation as Section 4.1. To solve the optimization problem in Equation (1), we solve three consecutive optimization sub-problems. In the first step, Equation (2), we approximately find a near-optimal solution for **sparse logistic regression** sparsity and box constraints, denoted as λ and (\mathbf{a}, \mathbf{b}) , respectively.

$$\begin{aligned}
 (\mathbf{w}^{(*)}, w_0^{(*)}) \in \arg \min_{\mathbf{w}, w_0} \mathcal{L}(\mathbf{w}, w_0, \mathcal{D}) &= \sum_{i=1}^n \log(1 + \exp(-y_i (\tilde{\mathbf{x}}_i^\top \mathbf{w} + w_0))) \\
 \text{s.t. } \|\mathbf{w}\|_0 &\leq \lambda, \mathbf{w} \in \mathbb{R}^p, w_0 \in \mathbb{R} \\
 \forall j \in [p], w_j &\in [a_j, b_j] \\
 \sum_{k=1}^{\Gamma} \mathbb{I}\{\mathbf{w}_{G_k} \neq \mathbf{0}\} &\leq \gamma.
 \end{aligned} \tag{2}$$

Solving Equation (2) produces an accurate and sparse *real-valued* solution $(\mathbf{w}^{(*)}, w_0^{(*)})$ that satisfies both feature and group sparsity constraints.

In the second step, we aim to produce multiple *real-valued* **near-optimal sparse logistic regression solutions under group sparsity constraint**, which is formulated as:

$$\begin{aligned}
 (\mathbf{w}^{(t)}, w_0^{(t)}) \text{ obeys } \mathcal{L}(\mathbf{w}^{(t)}, w_0^{(t)}, \mathcal{D}) &\leq \mathcal{L}(\mathbf{w}^{(*)}, w_0^{(*)}, \mathcal{D})(1 + \epsilon_u) \\
 \text{s.t. } \|\mathbf{w}^{(t)}\|_0 &\leq \lambda, \mathbf{w}^{(t)} \in \mathbb{R}^p, w_0^{(t)} \in \mathbb{R} \\
 \forall j \in [p], w_j^{(t)} &\in [a_j, b_j] \\
 \sum_{k=1}^{\Gamma} \mathbb{I}\{\mathbf{w}_{G_k}^{(t)} \neq \mathbf{0}\} &\leq \gamma.
 \end{aligned} \tag{3}$$

In particular, in order to solve Equation (3), we delete a feature j_- with support in $\text{supp}(\mathbf{w}^{(*)})$ and add a new feature with index j_+ . This procedure is repeated to turn the solution $(\mathbf{w}^{(*)}, w_0)$ into diverse sparse solutions with similar logistic loss. Note that during swapping, we only consider the alternative features that obey various constraints (including box constraint, groups-sparsity constraint, and monotonicity constraint) to ensure the new solutions are valid models.

$$\text{Find all } j_+ \text{ s.t. } \min_{\delta \in [a_{j_+}, b_{j_+}]} \mathcal{L}(\mathbf{w}^{(*)} - w_{j_-}^{(*)} \mathbf{e}_{j_-} + \delta \mathbf{e}_{j_+}, w_0, \mathcal{D}) \leq \mathcal{L}(\mathbf{w}^{(*)}, w_0^{(*)}, \mathcal{D})(1 + \epsilon_u). \tag{4}$$

We solve Equation (3) several times (set by the user as a hyper-parameter), after which we have a pool of distinct, almost-optimal sparse logistic regression models, and the top M models with the smallest logistic loss are selected, creating M solutions $\{(\mathbf{w}^{(t)}, w_0^{(t)})\}_{t=1}^M$. Note that the user can set ϵ_u and M arbitrarily, controlling the tolerance in logistic loss and the desired maximum quantity of diverse sparse solutions.

Lastly, for each solution in $\{(\mathbf{w}^{(t)}, w_0^{(t)})\}_{t=1}^M$, we compute an **integer risk score**, $(\mathbf{w}^{(+t)}, w_0^{(+t)})$, by performing rounding to a *real-valued* solution:

$$\begin{aligned}
 \mathcal{L}(\mathbf{w}^{(+t)}, w_0^{(+t)}, \mathcal{D}/m^{(t)}) &\leq \mathcal{L}(\mathbf{w}^{(t)}, w_0^{(t)}, \mathcal{D}) + \epsilon_t \\
 \text{s.t. } \mathbf{w}^{(+t)} &\in \mathbb{Z}^p, w_0^{(+t)} \in \mathbb{Z} \\
 \forall j \in [p], w_j^{(+t)} &\in [a_j, b_j] \\
 \sum_{k=1}^{\Gamma} \mathbb{I}\{\mathbf{w}_{G_k}^{(+t)} \neq \mathbf{0}\} &\leq \gamma.
 \end{aligned} \tag{5}$$

where ϵ_t is a gap in logistic loss with the near-optimal solution due to rounding. A theoretical upper bound on ϵ_t was proven in [29]. In order to round the coefficients, we perform the following steps: 1) we define

the largest multiplier m_{\max} as $\max\{\|\mathbf{a}\|_{\infty}, \|\mathbf{b}\|_{\infty}\}/\|\mathbf{w}^{(*)}\|_{\infty}$, and the smallest multiplier m_{\min} to be 1. 2) we select N_m equally spaced values within the range $[m_{\min}, m_{\max}]$, giving us a set of multipliers. 3) Using this set of multipliers, we scale the dataset, obtaining $\{1/m, \tilde{\mathbf{x}}_i/m, y_i\}_{i=1}^n$. 4) We send the scaled dataset to the sequential rounding algorithm [28, 29], which rounds the coefficients one at a time to an integer that best maintains accuracy (not necessarily the nearest integer). We use the integer coefficients and multiplier with the smallest logistic loss as our final solution.

C Additional Experiments

C.1 Source of Gains for Risk Score Generation

In this section, we perform an ablation study on the usefulness of our added functionality. Specifically, we run two sets of experiments: (1) vanilla FasterRisk [29] without group sparsity constraint nor monotonicity correction. (2) GROUPFASTERRISK with group sparsity constraint but without monotonicity correction. We present our results in terms of both tables (for quantitative measure of performances, see Table 4) and visualized risk scorecards (for qualitative measure of interpretability, see Figure 13 – Figure 21 in Appendix C.5).

Table 4: Ablation study on monotonicity correction. The evaluation is performed OOD on eICU. We observed a performance boost when monotonicity correction was applied, likely because correct domain information was included in the individual component scores of the features (see risk scorecard visualizations below).

		Sparse				Not Sparse		
		GFR-10 $F = 10$	OASIS $F = 10$	GFR-15 $F = 15$	SAPS II $F = 17$	GFR-40 $F = 40$	APACHE IV $F = 142$	APACHE IVa $F = 142$
With monotonicity correction	AUROC	0.844	0.805	0.859	0.844	0.864	0.871	0.873
	AUPRC	0.436	0.361	0.476	0.433	0.495	0.487	0.489
No monotonicity correction	AUROC	0.840	0.805	0.857	0.844	0.863	0.871	0.873
	AUPRC	0.427	0.361	0.467	0.433	0.491	0.487	0.489

C.2 Performance Comparisons

Table 5: GROUPFASTERRISK (not corrected with monotonicity constraints) compared with severity of illness scores under different group sparsity constraints. Evaluated on the internal MIMIC III dataset using 5-fold cross-validation, the best model from GROUPFASTERRISK is then evaluated OOD on the eICU dataset.

- Hosmer-Lemeshow χ^2 goodness of fit test, calculated using C statistic (10 bins created from deciles of predicted probabilities) [38].
- APACHE IV/IVa cannot be calculated on MIMIC III due to a lack of information for admission diagnoses.

		Moderate Sparsity				Not Sparse		
		GFR-10 $F = 10$	OASIS $F = 10$	GFR-15 $F = 15$	SAPS II $F = 17$	GFR-40 $F = 40$	APACHE IV $F = 142$	APACHE IVa $F = 142$
MIMIC III	AUROC	0.813 ± 0.007	0.775 ± 0.008	0.836 ± 0.006	0.795 ± 0.009	0.858 ± 0.008		
Test Folds	AUPRC	0.368 ± 0.011	0.314 ± 0.014	0.403 ± 0.011	0.342 ± 0.012	0.443 ± 0.013		
	Brier Score	0.079 ± 0.001	0.086 ± 0.001	0.077 ± 0.001	0.102 ± 0.001	0.074 ± 0.001		
	HL ^a χ^2	16.28 ± 2.51	146.16 ± 10.27	26.73 ± 6.38	691.45 ± 18.64	35.78 ± 11.01		
	SMR	0.992 ± 0.022	0.686 ± 0.008	0.996 ± 0.015	0.485 ± 0.005	1.002 ± 0.017		
eICU	AUROC	0.840	0.805	0.857	0.844	0.863	0.871	0.873
Test Set	AUPRC	0.427	0.361	0.467	0.433	0.491	0.487	0.489

Table 6: Performance comparison with machine learning methods, evaluated using 5-fold nested cross-validation on MIMIC III dataset, the best model is evaluated out-of-sample on eICU dataset.
a. Hosmer-Lemeshow χ^2 goodness of fit test, calculated using C statistic [38].

		GROUPFASTERRISK	EBM	XGBoost	AdaBoost	Random Forest	LogReg (ℓ_1)	LogReg (ℓ_2)
MIMIC III	AUROC	0.857 \pm 0.008	0.871 \pm 0.006	0.886 \pm 0.005	0.870 \pm 0.006	0.879 \pm 0.004	0.863 \pm 0.017	0.868 \pm 0.006
Test Folds	AUPRC	0.443 \pm 0.013	0.476 \pm 0.016	0.514 \pm 0.022	0.472 \pm 0.015	0.493 \pm 0.012	0.458 \pm 0.037	0.475 \pm 0.020
	Brier Score	0.074 \pm 0.001	0.071 \pm 0.001	0.073 \pm 0.002	0.215 \pm 0.0002	0.071 \pm 0.001	0.072 \pm 0.003	0.071 \pm 0.002
	HL χ^2	38.71 \pm 13.88	27.69 \pm 7.81	1569.00 \pm 616.82	3488.69 \pm 28.79	67.02 \pm 10.43	30.01 \pm 12.74	22.97 \pm 4.42
	SMR	1.006 \pm 0.018	1.013 \pm 0.013	1.858 \pm 0.087	0.226 \pm 0.0003	0.996 \pm 0.008	1.000 \pm 0.014	1.002 \pm 0.019
eICU	AUROC	0.863	0.878	0.885	0.878	0.883	0.870	0.871
Test Set	AURPC	0.491	0.511	0.525	0.509	0.517	0.496	0.507
	Brier Score	0.068	0.062	0.065	0.219	0.063	0.063	0.063
	HL χ^2	3253.75	443.64	65437.29	68054.18	2220.83	315.65	885.87
	SMR	0.664	0.856	1.786	0.199	0.780	0.876	0.798

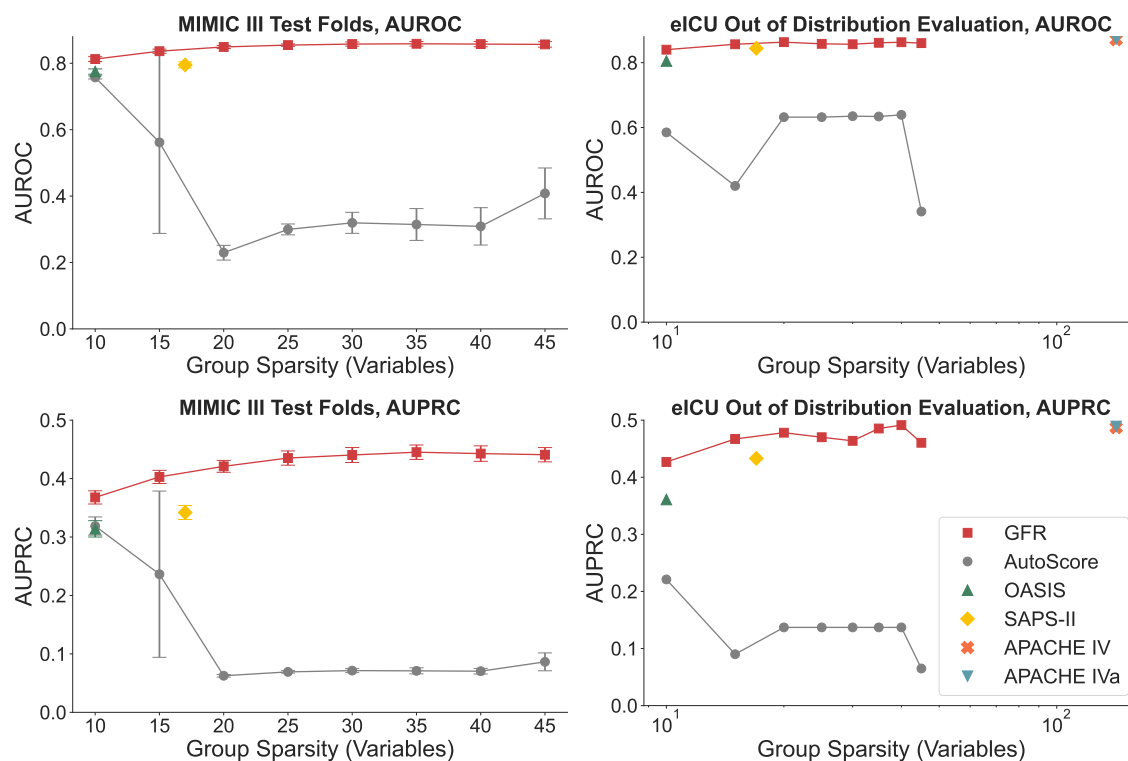


Figure 9: Performance of GROUPFASTERRISK under various values of group sparsity. We added a comparison with AutoScore [26] as an additional baseline. AutoScore is another automatic risk scorecard generation framework. At a high level, AutoScore creates risk scores by scaling logistic regression coefficients by the smallest of its real-valued coefficients, and it rounds coefficient values to the nearest integer afterward. A fine-tuning stage could be used by practitioners to adjust learned integer coefficients. We trained multiple AutoScore and GROUPFASTERRISK models at various group sparsity levels (number of features) and compared their performances. We found that GROUPFASTERRISK consistently outperformed AutoScore across all levels of group sparsity. AutoScore sometimes produces solutions where the AUROC is less than 0.5, which means that lower risk scores would actually imply higher risk outcomes, which is unintuitive. These observations show that without using the multiplier trick and smart rounding techniques, solutions tend to have poor qualities.

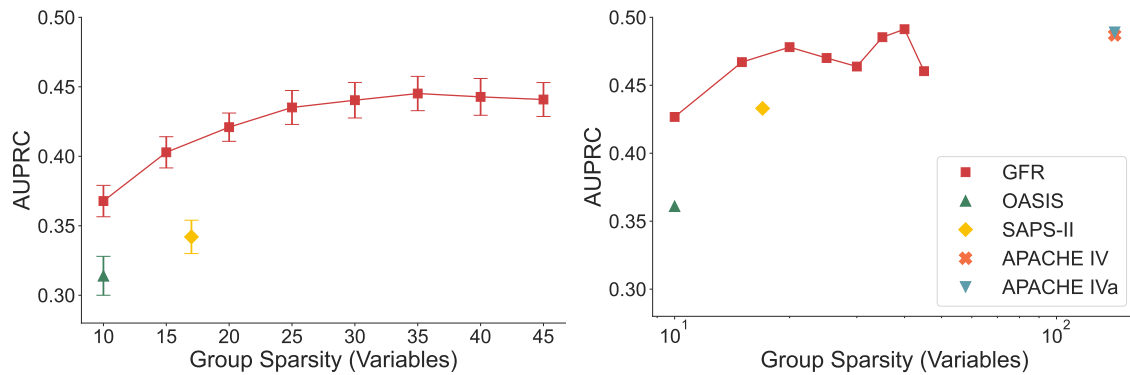
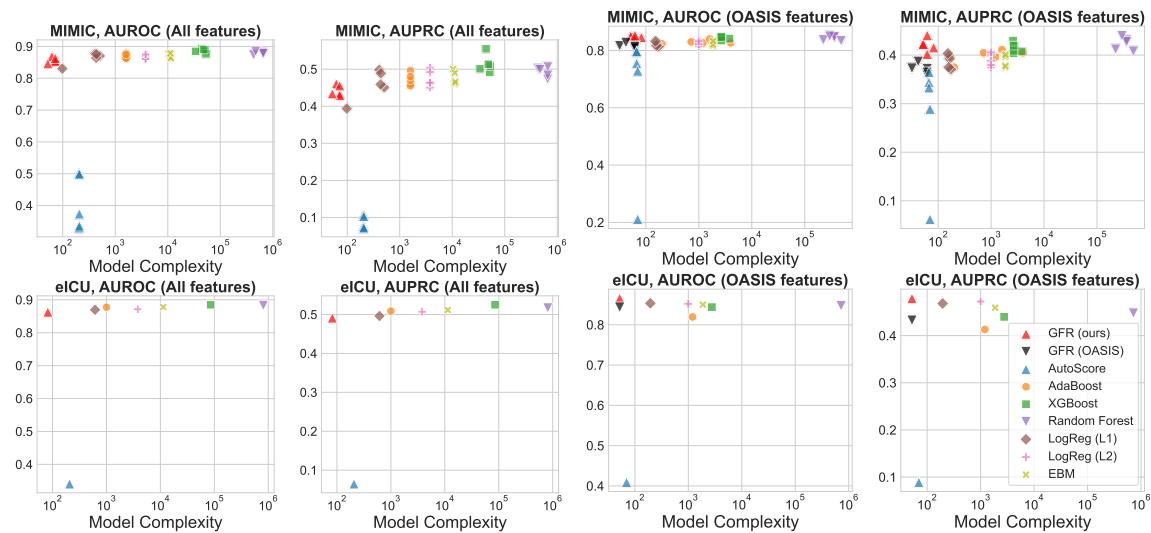


Figure 10: Performance under different group sparsities measured by AUPRC (without AutoScore). In this figure, we use AUPRC as the metric, which is different from Figure 4a that uses AUROC as the metric.

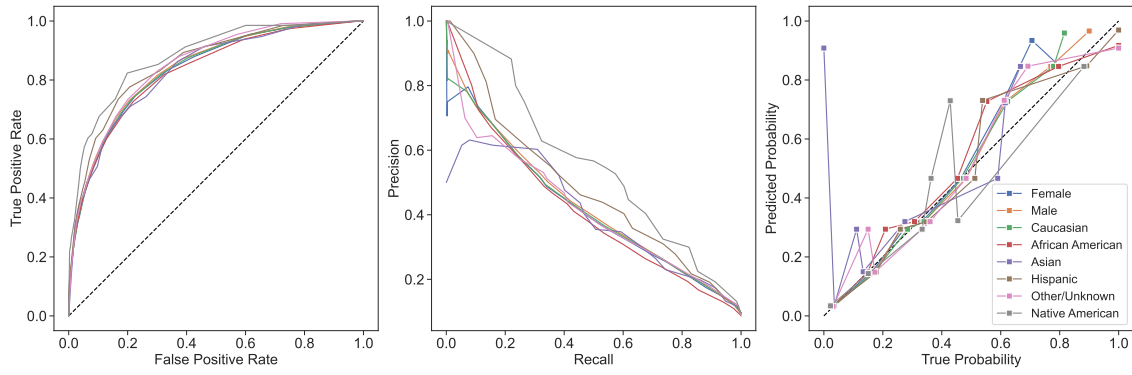


(a) Using all features.

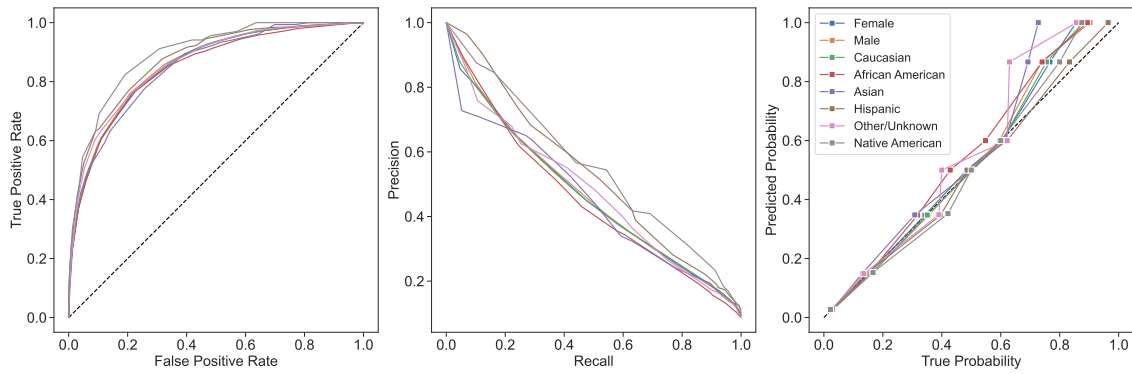
(b) Using OASIS features.

Figure 11: Complexity graph, GFR vs. ML algorithms. In this figure, GFR (ours) uses 19 variables, which is different from 14 variables used for Figure 7.

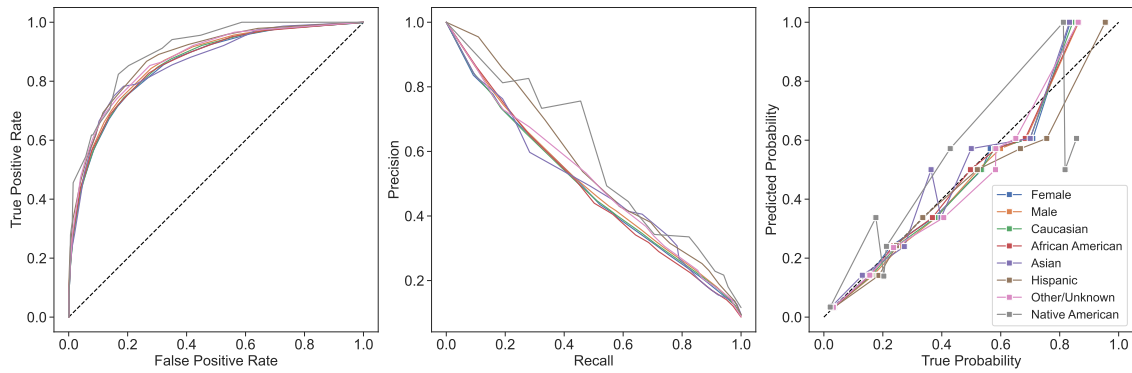
C.3 Fairness and Calibration Evaluations



GFR-10 Fairness Performance.



GFR-15 Fairness Performance.



GFR-40 Fairness Performance.

Table 7: Out of distribution performance comparison with existing baselines. GROUPFASTERRISK is trained on disease-specific MIMIC subpopulation using various group sparsity constraints. We believe the drop in performance on the OOD on the eICU dataset is due to limited training data size on the MIMIC III sub-populations. Specifically, there are about 6,407 patients for acute kidney failure, 6,983 for heart failure, 3,505 for sepsis, and 3,625 for acute myocardial infarction, which is not enough to construct high-quality risk scores.

		Low Sparsity			Moderate Sparsity		Not Sparse		
		GFR-10 $F = 10$	OASIS $F = 10$	SOFA $F = 11$	GFR-15 $F = 15$	SAPS II $F = 17$	GFR-40 $F = 40$	APACHE IV $F = 142$	APACHE IVa $F = 142$
Sepsis/Septicemia	AUROC	0.684	0.734	0.726	0.720	0.782	0.696	0.780	0.781
	AUPRC	0.423	0.435	0.461	0.459	0.512	0.425	0.504	0.503
Acute Myocardial Infarction	AUROC	0.858	0.846	0.795	0.814	0.879	0.785	0.879	0.886
	AUPRC	0.409	0.424	0.395	0.375	0.493	0.342	0.493	0.498
Heart Failure	AUROC	0.745	0.731	0.702	0.730	0.770	0.742	0.782	0.787
	AUPRC	0.352	0.351	0.337	0.326	0.396	0.328	0.423	0.425
Acute Kidney Failure	AUROC	0.739	0.760	0.723	0.763	0.781	0.765	0.803	0.802
	AUPRC	0.485	0.472	0.462	0.479	0.527	0.511	0.552	0.550

Table 8: Fairness and calibration results across sub-groups in eICU study cohort. All models are calibrated using isotonic regression on 2,000 patients in the eICU cohort population, and evaluation is performed on the remaining population. Recall that in Table 1, we only calibrated GROUPFASTERRISK.

		Ethnicity (alphabetical order)						Gender	
		African American	Asian	Caucasian	Hispanic	Native American	Other/Unknown	Female	Male
AUROC	GFR-10	0.829	0.833	0.837	0.856	0.881	0.849	0.835	0.840
	OASIS	0.811	0.797	0.803	0.825	0.824	0.809	0.806	0.805
	GFR-15	0.846	0.848	0.854	0.873	0.895	0.860	0.853	0.856
	SAPS II	0.846	0.828	0.843	0.859	0.893	0.842	0.844	0.845
	GFR-40	0.859	0.861	0.859	0.881	0.902	0.873	0.857	0.865
	APACHE IVa	0.875	0.866	0.870	0.893	0.901	0.886	0.869	0.876
AUPRC	GFR-10	0.415	0.390	0.422	0.480	0.558	0.418	0.418	0.429
	OASIS	0.345	0.330	0.364	0.410	0.370	0.328	0.356	0.365
	GFR-15	0.453	0.454	0.466	0.534	0.555	0.477	0.466	0.471
	SAPS II	0.424	0.408	0.435	0.470	0.598	0.395	0.440	0.428
	GFR-40	0.488	0.500	0.489	0.553	0.585	0.512	0.488	0.499
	APACHE IVa	0.487	0.492	0.487	0.538	0.522	0.484	0.481	0.496
Brier Score	GFR-10	0.064	0.070	0.068	0.065	0.059	0.065	0.068	0.067
	OASIS	0.068	0.076	0.072	0.069	0.071	0.070	0.072	0.070
	GFR-15	0.062	0.068	0.065	0.061	0.059	0.061	0.065	0.064
	SAPS II	0.064	0.071	0.068	0.065	0.057	0.067	0.067	0.067
	GFR-40	0.060	0.064	0.064	0.060	0.057	0.059	0.064	0.062
	APACHE IVa	0.060	0.067	0.064	0.059	0.061	0.061	0.064	0.062
HL χ^2	GFR-10	27.90	11.00	113.70	24.68	5.48	12.53	58.65	102.74
	OASIS	12.89	19.16	41.68	13.47	4.39	8.19	26.37	25.26
	GFR-15	23.64	9.88	63.40	10.62	4.43	3.73	13.62	57.75
	SAPS II	70.37	19.94	193.09	21.58	6.28	44.37	118.68	130.72
	GFR-40	8.72	5.20	120.03	12.03	11.57	6.09	58.34	97.92
	APACHE IVa	47.89	7.75	100.27	6.25	14.24	19.45	78.47	46.56
SMR	GFR-10	0.946	0.915	1.028	1.017	0.949	1.013	0.993	1.031
	OASIS	0.952	1.276	1.000	1.069	0.928	1.075	0.995	1.014
	GFR-15	0.974	0.921	1.040	1.046	1.003	0.996	1.002	1.046
	SAPS II	0.941	1.096	0.986	1.082	0.950	1.056	1.004	0.981
	GFR-40	1.022	0.936	1.039	1.063	0.889	1.033	1.000	1.058
	APACHE IVa	0.891	0.997	1.003	0.962	0.792	0.952	0.983	0.988

C.4 GROUPFASTERRISK Performances

Table 9: GROUPFASTERRISK performance under various bin widths. To allow GROUPFASTERRISK to better utilize continuous variables, a binarization technique is applied, which transforms a continuous variable into B quantiles (bins). The experiment is conducted using 5 fold cross validation on MIMIC III training and validation folds; each cross validation gives a mean AUROC and AUPRC. Each B represents a fixed combination of group sparsity and sparsity constraints, and the mean and standard deviation of all those runs is reported.

Number of Bins (B)		100	50	20	10	5	4
Average Mean AUROC	Training	0.847 \pm 0.030	0.849 \pm 0.029	0.856 \pm 0.020	0.850 \pm 0.023	0.847 \pm 0.016	0.841 \pm 0.019
	Validation	0.828 \pm 0.030	0.832 \pm 0.028	0.843 \pm 0.018	0.839 \pm 0.022	0.840 \pm 0.015	0.835 \pm 0.018
Average Mean AUPRC	Training	0.444 \pm 0.057	0.448 \pm 0.056	0.451 \pm 0.043	0.439 \pm 0.046	0.430 \pm 0.032	0.413 \pm 0.036
	Validation	0.394 \pm 0.047	0.401 \pm 0.047	0.414 \pm 0.033	0.413 \pm 0.037	0.412 \pm 0.028	0.401 \pm 0.032

C.5 Visualizations of Risk Scores Generated by GROUPFASTERRISK

In this section, we present the risk scores generated by GROUPFASTERRISK for group sparsity of 10, 15, 40 (Appendix C.5.1) as well as visualize the score cards a part of our ablation study discussed in Appendix C.1. Specifically, we present three sets of risk scores to highlight the usefulness of group sparsity and monotonicity constraints:

1. Risk scores generated with **both group sparsity and monotonicity constraints**, Appendix C.5.1. These models correspond to those produced by GROUPFASTERRISK.
2. Risk scores generated with **neither group sparsity nor monotonicity constraints**, Appendix C.5.2. Here, we do not optimize for group sparsity constraints γ that we discussed in Section 4.1 and do not apply monotonic correction (Section 4.4).
3. Risk scores generated with **only group sparsity and without monotonicity constraints**, Appendix C.5.3. Here, we do not apply monotonic correction that we discussed in Section 4.4.

For each set, we use group sparsity of 10, 15, and 40. In Appendix C.5.1, for risk scores with group sparsity of 10, we apply monotonicity constraints on *Max Bilirubin*, *Min GCS*, and *Min SBP*. For a group sparsity of 15, we apply monotonicity constraints on *Max Bilirubin*, *Min GCS*, *Min SBP*, and *Max BUN*. For a group sparsity of 40, we apply monotonicity constraints on *Max Bilirubin*, *Max Sodium*, *Min Respiratory Rate*, and *Min Bicarbonate*.

We observe that the addition of group sparsity constraints allows us to create more cohesive risk scores, and monotonicity constraints allow for the inclusion of medical domain knowledge into the risk score. For instance, when not using monotonicity constraints, we observe that the model creates risk scores that predict a lower risk for patients with minimum Glasgow Coma Score (GCS) of 3 than those with higher minimum GCS. This is partly due to the training dataset, which has fewer samples with minimum GCS of 3 than those with minimum GCS between 3 and 6. Thus, this relationship is often reflected by models trained without monotonicity constraints. Luckily, due to the interpretable nature of our model, we can notice this easily and apply monotonicity constraints to correct it.

C.5.1 With both group sparsity and monotonicity constraints

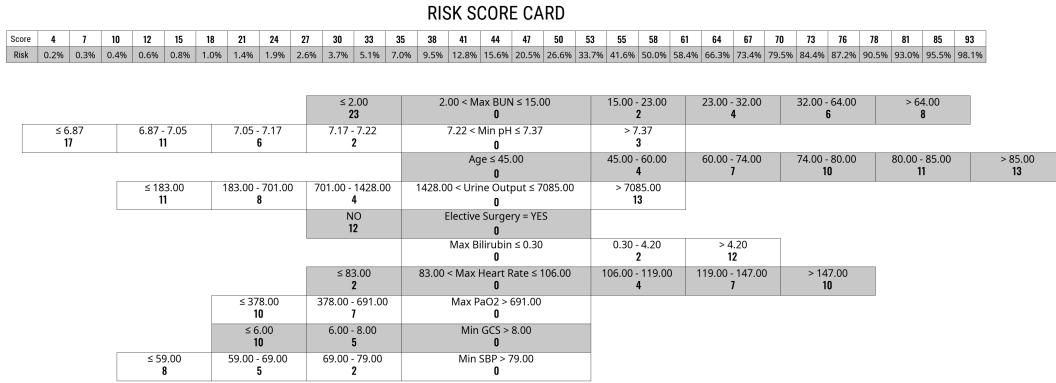


Figure 13: With group sparsity of 10. Both group sparsity and monotonicity constraints are applied.

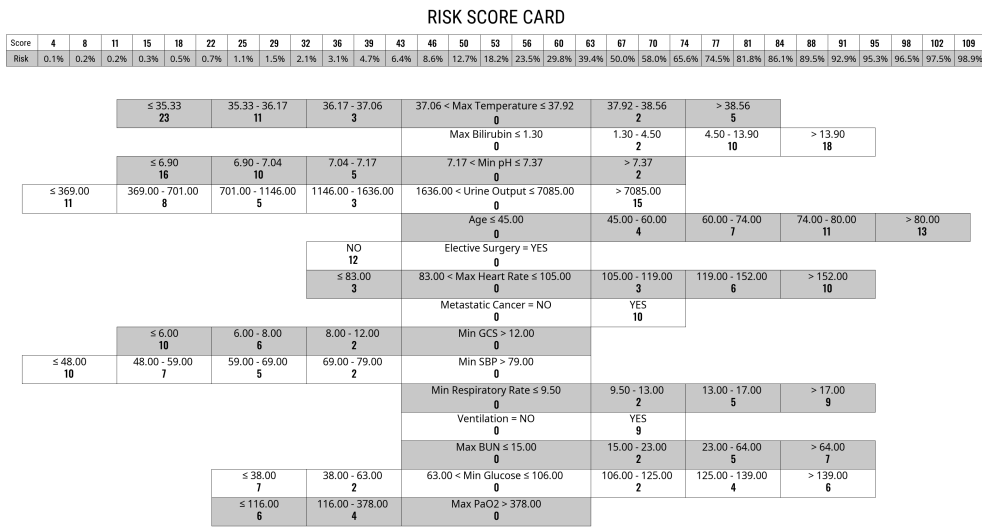


Figure 14: With group sparsity of 15. Both group sparsity and monotonicity constraints are applied.

RISK SCORE CARD

Score	19	29	43	50	58	66	77	85	104	120	128	135	142	149	157	164	171	178	185	193	200	207	214	222	229	236	243	251	258	272
Risk	0.0%	0.0%	0.1%	0.1%	0.2%	0.2%	0.4%	0.6%	1.0%	1.6%	2.5%	4.0%	6.2%	9.5%	13.3%	19.7%	28.1%	38.5%	50.0%	61.5%	71.9%	80.3%	86.7%	91.2%	94.3%	96.0%	97.5%	98.4%	99.1%	99.6%

≤ 0.30 34	0.30 - 2.80 26	2.80 - 4.80 22	4.80 - 9.70 14	Max Sodium ≤ 118.00 0	118.00 - 143.00 55	143.00 - 146.00 58	146.00 - 154.00 62	> 154.00 72
				Max Creatinine > 9.70 0				
			≤ 2.00 29	2.00 < Max BUN ≤ 23.00 0	> 23.00 4			
	≤ 128.00 24	128.00 - 145.00 18	145.00 - 151.00 13	Min Sodium > 151.00 0				
		≤ 82.00 22	82.00 - 718.00 14	Max Glucose > 718.00 0				
		≤ 12.70 11	12.70 - 51.60 20	Min Bilirubin > 51.60 0				
≤ 183.00 19	183.00 - 701.00 11	701.00 - 1146.00 7	1146.00 - 1636.00 4	1636.00 < Urine Output ≤ 7540.00 0	> 7540.00 16			
				Age ≤ 45.00 0	45.00 - 59.00 5	59.00 - 74.00 9	74.00 - 80.00 13	> 80.00 16
≤ 33.00 14	33.00 - 34.39 8	34.39 - 35.89 3		Min Temperature > 35.89 0				
				Min Potassium ≤ 4.20 0	4.20 - 5.40 3	> 5.40 13		
≤ 6.99 12	6.99 - 7.17 4			Min pH > 7.17 0				
		≤ 86.00 3	86.00 < Max Heart Rate ≤ 105.00 0	105.00 - 119.00 3	119.00 - 157.00 6	> 157.00 11		
				Min BUN ≤ 51.00 0	51.00 - 86.00 5	> 86.00 11		
				Min WBC ≤ 12.50 0	12.50 - 31.60 4	> 31.60 11		
		≤ 7.15 11	7.15 < Max pH ≤ 7.47 0	> 7.47 3				
				Metastatic Cancer = NO 0	YES 11			
				Ventilation = NO 0	YES 10			
≤ 6.00 10	6.00 - 8.00 5			Min GCS > 8.00 0				
		NO 10		Elective Surgery = YES 0				
		≤ 29.00 9	29.00 < Min Glucose ≤ 122.00 0	122.00 - 139.00 3	> 139.00 6			
				Hematologic Cancer = NO 0	YES 9			
≤ 3.60 9	3.60 - 23.80 4			Max WBC > 23.80 0				
				Max Bilirubin ≤ 4.20 0	> 4.20 9			
		≤ 36.17 9	36.17 < Max Temperature ≤ 38.56 0	> 38.56 4				
≤ 110.00 9	110.00 - 122.00 4			122.00 < Max SBP ≤ 151.00 0	151.00 - 187.00 2	> 187.00 5		
				Min Respiratory Rate ≤ 9.50 0	9.50 - 13.00 2	13.00 - 18.00 5	> 18.00 8	
		≤ 1.50 8	1.50 < Min Albumin ≤ 1.50 0	> 1.50 7				
		≤ 40.00 4	40.00 < Pre-ICU LOS ≤ 11517.00 0	> 11517.00 7				
≤ 116.00 5	116.00 - 378.00 3			Max PaO2 > 378.00 0				
				Min Hematocrit ≤ 29.20 0	> 29.20 4			
		≤ 69.00 4	69.00 < Min SBP ≤ 69.00 0	> 69.00 4				
		≤ 30.50 4	30.50 < Max Hematocrit ≤ 30.50 0	> 30.50 4				
		≤ 157.78 3	157.78 < Min P/F Ratio ≤ 157.78 0	> 157.78 3				
		≤ 31.00 3	31.00 < Min PaCO2 ≤ 31.00 0	> 31.00 3				
		≤ 39.67 3	39.67 < Min MBP ≤ 39.67 0	> 39.67 3				
		≤ 4.30 3	4.30 < Max Potassium ≤ 4.30 0	> 4.30 3				
		≤ 38.00 3	38.00 < Max PaCO2 ≤ 38.00 0	> 38.00 3				
		≤ 2.40 3	2.40 < Max Albumin ≤ 2.40 0	> 2.40 3				
		≤ 658.00 3	658.00 < aado2_max ≤ 658.00 0	> 658.00 3				
				Max Respiratory Rate ≤ 31.00 0	> 31.00 2			

Figure 15: With group sparsity of 40. Both group sparsity and monotonicity constraints are applied.

C.5.2 With neither group sparsity nor monotonicity constraints

We trained GROUPFASTERRISK models without group sparsity and monotonicity constraints to indicate the usefulness of these functionalities in risk score generation. For direct and fair comparisons, we set all of the hyperparameters (other than γ and (a, b)) the same as those used in Appendix C.5.1.

Observe that the risk scores are less cohesive (more features, fewer options per feature) than the ones trained with group sparsity constraints. In particular, the user loses control over the total number of component functions for the risk score. Additionally, without monotonicity, the component functions may reflect noise in the data that does not align with domain knowledge. For instance, Figure 18 has a risk score that decreases even when *Min Respiratory Rate* is dangerously low.

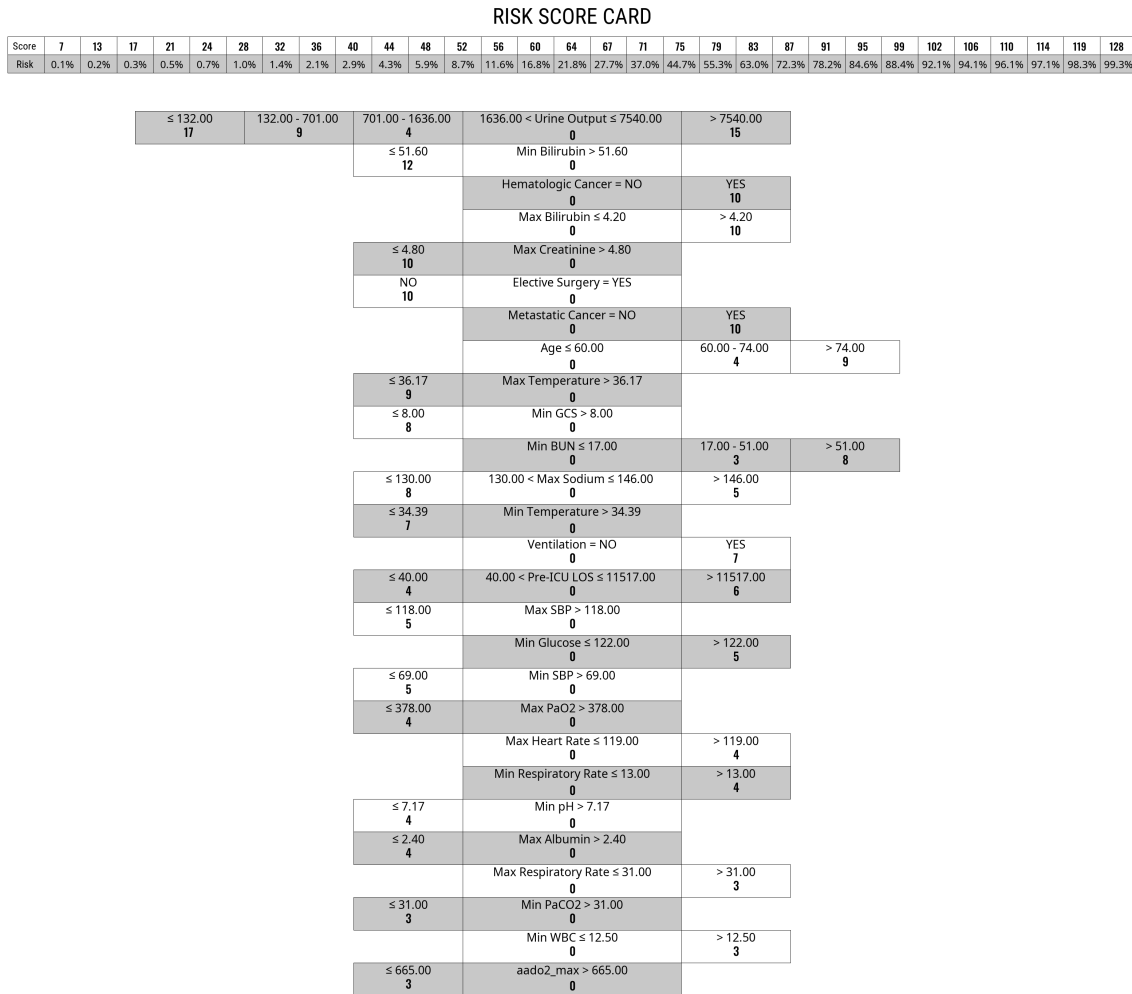


Figure 16: With the same hyperparameters as the previous model with group sparsity of 10 in Appendix C.5.1. Neither group sparsity nor monotonicity constraints are applied.

RISK SCORE CARD

Score	16	20	25	30	35	40	44	49	53	58	63	67	72	76	81	86	90	95	99	104	109	113	118	122	127	132	136	141	145	163
Risk	0.1%	0.1%	0.2%	0.3%	0.5%	0.7%	1.0%	1.6%	2.4%	3.5%	5.1%	7.4%	10.5%	14.8%	20.4%	27.4%	35.8%	45.1%	54.9%	64.2%	72.6%	79.6%	86.4%	90.4%	93.3%	95.3%	96.8%	97.8%	98.5%	99.7%

≤ 6.98 20 18	6.98 - 7.17 11 10	7.17 - 7.61 7 4	Min pH > 7.61 0	1636.00 < Urine Output ≤ 7540.00 0	> 7540.00 17
			Age ≤ 45.00 0	45.00 - 60.00 5	60.00 - 74.00 9
	≤ 4.20 2	4.20 - 55.50 13	Max Bilirubin > 55.50 0		
		≤ 4.80 11	Max Creatinine > 4.80 0		
		≤ 718.00 11	Max Glucose > 718.00 0		
			Metastatic Cancer = NO 0	YES 11	
			Hematologic Cancer = NO 0	YES 10	
		NO 10	Elective Surgery = YES 0		
		≤ 36.17 9	36.17 < Max Temperature ≤ 38.56 0	> 38.56 3	
≤ 34.39 9	34.39 - 35.89 2		Min Temperature > 35.89 0		
		≤ 1.50 9	Min Albumin > 1.50 0		
		≤ 130.00 8	130.00 < Max Sodium ≤ 146.00 0	> 146.00 5	
			Ventilation = NO 0	YES 8	
		≤ 8.00 8	Min GCS > 8.00 0		
		≤ 40.00 4	40.00 < Pre-ICU LOS ≤ 11517.00 0	> 11517.00 7	
			Min Respiratory Rate ≤ 13.00 0	13.00 - 18.00 4	> 18.00 7
			Min BUN ≤ 51.00 0	> 51.00 6	
			Min Glucose ≤ 122.00 0	> 122.00 5	
		≤ 118.00 5	118.00 < Max SBP ≤ 187.00 0	> 187.00 3	
		≤ 69.00 4	Min SBP > 69.00 0		
			Min Potassium ≤ 4.20 0	> 4.20 4	
			Max Heart Rate ≤ 119.00 0	> 119.00 4	
			Min Hematocrit ≤ 29.20 0	> 29.20 4	
		≤ 30.50 4	Max Hematocrit > 30.50 0		
		≤ 2.40 4	Max Albumin > 2.40 0		
			Max pH ≤ 7.47 0	> 7.47 4	
			Min WBC ≤ 12.50 0	> 12.50 3	
			Max BUN ≤ 23.00 0	> 23.00 3	
			Max Respiratory Rate ≤ 31.00 0	> 31.00 3	
		≤ 108.33 3	Min P/F Ratio > 108.33 0		
		≤ 39.67 3	Min MBP > 39.67 0		
		≤ 38.00 3	Max PaCO2 > 38.00 0		
		≤ 4.30 3	Max Potassium > 4.30 0		
		≤ 665.00 3	aado2_max > 665.00 0		
		≤ 31.00 2	Min PaCO2 > 31.00 0		

Figure 17: With the same hyperparameters as the previous model with group sparsity of 15 in Appendix C.5.1. Neither group sparsity nor monotonicity constraints are applied.

RISK SCORE CARD

Score	24	33	41	48	56	64	72	79	105	115	124	132	139	146	153	161	168	175	183	190	197	205	212	219	227	234	241	248	256	269
Risk	0.0%	0.0%	0.0%	0.1%	0.1%	0.2%	0.3%	0.5%	0.8%	1.2%	2.0%	3.1%	4.8%	7.5%	11.4%	17.1%	24.7%	34.3%	45.4%	56.9%	67.8%	77.0%	82.9%	88.6%	92.5%	95.2%	96.9%	98.0%	99.1%	99.5%

	≤ 2.00	2.00 - 23.00	23.00 - 117.00	Max Sodium ≤ 118.00	118.00 - 130.00	130.00 - 143.00	143.00 - 146.00	146.00 - 154.00	154.00 - 170.00	> 170.00
	33	3	7	0	76	71	74	79	88	88
	≤ 0.30	0.30 - 2.80	2.80 - 4.80	Max BUN > 117.00						
		13	9	0						
		11	20	0						
		8	3	0						
	19	10	3	0						
		19	11	0						
				Age ≤ 45.00	45.00 - 60.00	60.00 - 74.00	74.00 - 80.00	> 80.00		
	15	8	3	0	5	9	13	16		
		14	4	0						
				Min Temperature > 35.89						
				Min pH > 7.17						
				Min BUN ≤ 51.00	51.00 - 86.00	> 86.00				
				Min Sodium > 145.00						
				Metastatic Cancer = NO	YES					
	5	8	11	0	11					
				Min Respiratory Rate > 25.00						
				Min WBC ≤ 12.50	12.50 - 32.10	> 32.10				
				Min GCS > 8.00						
	10	5		0						
				Elective Surgery = YES						
				Min Bicarbonate ≤ 8.00	8.00 - 15.00	> 15.00				
				Ventilation = NO	YES					
				Hematologic Cancer = NO	YES					
				36.17 < Max Temperature ≤ 38.56	> 38.56					
				Min Bilirubin ≤ 12.70	> 12.70					
				Min Potassium ≤ 4.20	4.20 - 5.10	> 5.10				
				29.00 < Min Glucose ≤ 122.00	122.00 - 139.00	> 139.00				
				Max WBC > 23.80						
				Min Albumin > 1.50						
				Max Heart Rate ≤ 119.00	119.00 - 157.00	> 157.00				
				40.00 < Pre-ICU LOS ≤ 11517.00	> 11517.00					
				Min PaCO2 > 31.00						
				Max PaO2 > 378.00						
				118.00 < Max SBP ≤ 187.00	> 187.00					
				Min Hematocrit ≤ 29.20	> 29.20					
				Max Hematocrit > 30.50						
				Min SBP > 69.00						
				Max Albumin > 2.40						
				Max PaCO2 > 38.00						
				Min Heart Rate ≤ 93.00	> 93.00					
				Min P/F Ratio > 108.33						
				Min MBP > 39.67						
				Max pH ≤ 7.47	> 7.47					
				Max Respiratory Rate ≤ 31.00	> 31.00					
				Max Potassium > 4.30						
				aado2_max > 665.00						

Figure 18: With the same hyperparameters as the previous model with group sparsity of 40 in Appendix C.5.1. Neither group sparsity nor monotonicity constraints are applied.

C.5.3 With only group sparsity and without monotonicity constraints

We trained GROUPFASTERRISK models with group sparsity but without monotonicity constraints. This enables us to see the usefulness of monotonicity correction. For direct and fair comparisons, we set all of the hyperparameters (other than (a, b)) the same as those used in Appendix C.5.1.

Observe that the model in Figure 19 predicts lower risk for patients with minimum GCS of 3 than those with minimum GCS between 3 and 6.

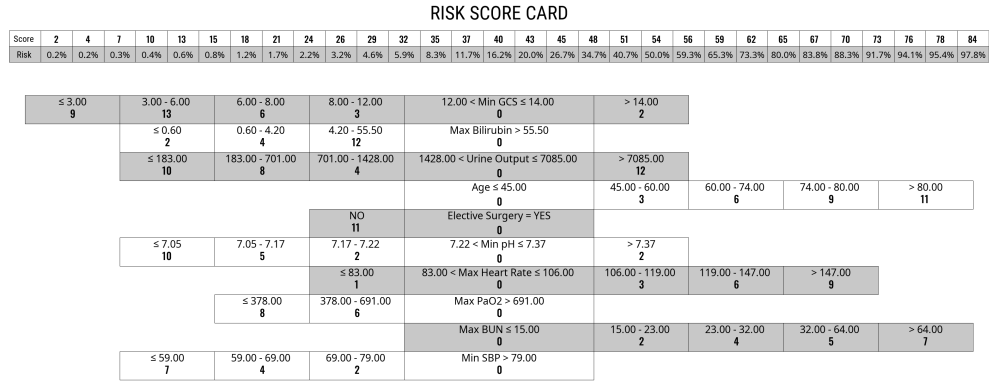


Figure 19: With group sparsity of 10. With group sparsity but without monotonicity constraints.

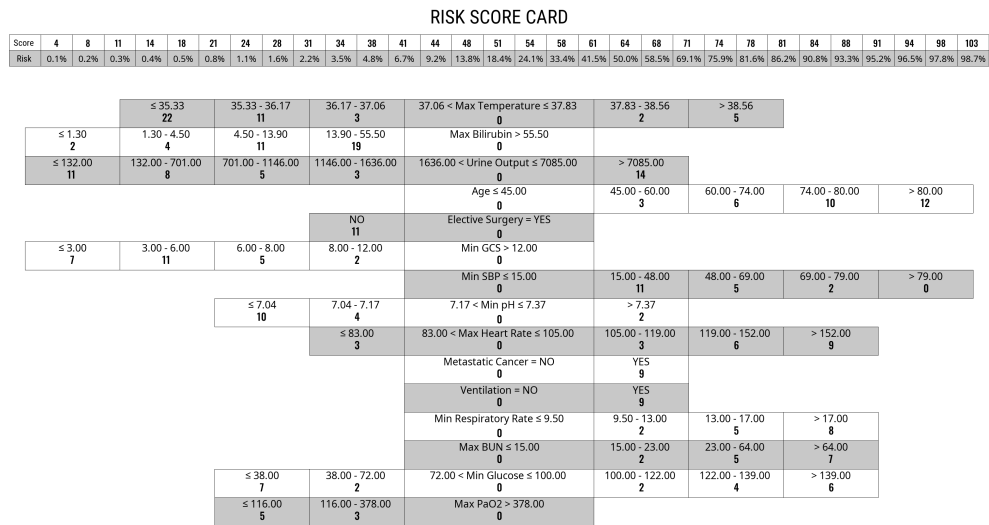


Figure 20: With group sparsity of 15. With group sparsity but without monotonicity constraints.

